Single-cell bisulfite sequencing of spermatozoa from lean and obese humans reveals potential for the transmission of epimutations

Emil Andersen[1], Stephen Clark[2], Lars Ingerslev[1], Leonidas Lundell[1], Wolf Reik[2] and Romain Barrès[1*]

[1] Novo Nordisk Foundation Center for Basic Metabolic Research, Faculty of Health and Medical Sciences, University of Copenhagen, Copenhagen, Denmark.

[2] Epigenetics Programme, The Babraham Institute, Babraham Research Campus, Cambridge, UK.

[*]**To whom correspondence should be addressed:**

Romain Barrès

Panum Institutet 7.7, Blegdamsvej 3B, 2200 Copenhagen N, Denmark.

Tel. +45 35 33 72 88

Fax. +45 35 33 71 01

Email: barres@sund.ku.dk

ABSTRACT

Epigenetic marks in gametes modulate developmental programming after fertilization. Spermatozoa from obese men exhibit distinct epigenetic signatures compared to lean men, however, whether epigenetic differences are concentrated in a sub-population of spermatozoa or spread across the ejaculate population is unknown. Here, by using whole-genome single-cell bisulfite sequencing on 87 motile spermatozoa from 8 individuals (4 lean and 4 obese), we found that spermatozoa within single ejaculates are highly heterogeneous and contain subsets of spermatozoa with marked imprinting defects. Comparing lean and obese subjects, we discovered methylation differences across two large CpG dense regions located near *PPM1D* and *LINC01237*. These findings confirm that sperm DNA methylation is altered in human obesity and indicate that single ejaculates contain subpopulations of spermatozoa carrying distinct DNA methylation patterns. Distinct epigenetic patterns of spermatozoa within an ejaculate may result in different intergenerational effects and therefore influence strategies aiming to prevent epigenetic-related disorders in the offspring.

INTRODUCTION

Spermatozoa carry a specific epigenetic signature that controls normal embryonic development (Aston et al., 2015; Hammoud et al., 2009) and abnormalities in the epigenetic pattern of sperm are associated with decreased fertility in humans and raise concern for potential epigenetic transmission to the offspring (Conine et al., 2018; Jenkins et al., 2016; Kaneda et al., 2004; Vasiliauskaitė et al., 2018). Methylation of DNA on the fifth carbon of cytosine (5mC) is an extensively studied epigenetic mark that controls gene expression in time and space, and for which accumulating evidence indicates a role in embryonic development (Peat et al., 2014; Tang et al., 2015).

Environmental challenges such as diet, physical exercise, toxins, and psychological stress can alter DNA methylation in gametes (Donkin and Barrès, 2018). Our group and others have shown that the DNA methylation signature of human spermatozoa is amenable to lifestyle influence, such as weight loss and endurance training (Denham et al., 2015; Donkin and Barrès, 2018; Donkin et al., 2016; Ingerslev et al., 2018). Environmentally induced epigenetic change in gametes, therefore, constitutes a plausible mechanism by which environmental factors before conception may influence the phenotype of the next generation. However, the functional consequences of environmentally induced spermatozoal DNA methylation on embryo development have not been elucidated.

As spermatozoa are haploid, methylation levels at a single CpG site directly correspond to the fraction of cells carrying a methyl group on that cytosine. Thus, environmentally induced DNA methylation changes at the single CpG dinucleotide that are smaller than 100% imply that only a fraction of cells in the ejaculate carry that change. For example, a modest increase in methylation on a single CpG site detected in a whole ejaculate from 20% to 40% implicates that an additional 20%

of spermatozoa carry a methyl group on that cytosine residue. It is currently unknown if environmentally induced DNA methylation changes across the genome are carried by a sub-population of spermatozoa or are spread across the ejaculate population in a mosaic-like fashion. This information will help to increase our understanding of the mechanisms by which the sperm epigenome is remodeled in response to environmental factors and may have implications for the field of assisted reproduction where selection of single spermatozoa is performed.

Recent developments in single-cell sequencing technologies have allowed for greater exploration of human development (Wen and Tang, 2019). Techniques such as single-cell reduced representation bisulfite sequencing (scRRBS) or post-bisulfite adaptor tagging (PBAT)-based single-cell bisulfite sequencing (scBS-seq) have now been used to profile the DNA methylome of human preimplantation embryos, as well as oocytes and sperm (Guo et al., 2015; Smallwood et al., 2014a; Zhou et al., 2019; Zhu et al., 2018). Although spermatozoal single-cell DNA methylation sequencing has been performed previously in two individuals (Guo et al., 2015; Zhu et al., 2018), it has been done to validate the technical feasibility of the method and to serve as a macroscopic comparison to the oocyte. A detailed DNA methylation profiling of spermatozoa has not been conducted to date.

Here, we performed an adapted PBAT scBS-seq analysis of human sperm cells at single-cell and single-base resolution to map the distribution of DNA methylation marks across cells of a single ejaculate as well as between individuals. We confirm DNA methylation differences between spermatozoa from lean and obese individuals and establish that spermatozoa within one ejaculate have distinct patterns and may harbor marked defects in methylation at specific imprinted loci. Our results provide novel insight into the heterogeneity of sperm DNA methylation in human ejaculates.

RESULTS

Post bisulfite adaptor tagging single-cell sequencing of spermatozoa

To compare the epigenetic profile of single spermatozoa from lean and obese individuals, we adapted our PBAT based scBS-seq to circumvent the dense packaging of spermatozoa (Clark et al., 2017; Smallwood et al., 2014b; Smith et al., 2012) by including an additional lysis step and a longer bisulfite conversion (see Methods) (Clark et al., 2017)(Figure 1A). In total, we sequenced 87 spermatozoa from 4 lean and 4 obese individuals at a sequencing depth averaging 15.93 million (M) 100 base-pair (bp) paired-end reads (range, 1.5M to 216.2M reads) (Table S1 and Figure 1B). Although our mapping rate was lower than somatic cells, it was consistent with a previous study using PBAT scBS-seq in spermatozoa (Table S1 and Figure 1C) (Clark et al., 2017; Smallwood et al., 2014b; Zhu et al., 2018). (Figure 1C). Our results are highly correlated with another dataset of spermatozoa (Zhu et al., 2018), but not with DNA methylation data of single oocytes (Zhu et al., 2018) (Figure 1D and Figure 1E). Plotting DNA methylation signals of single cell spermatozoa and oocytes by multi-dimensional scaling (MDS) also showed that this profiling of spermatozoal DNA methylation is specific and consistent with the literature (Figure 1F and Figure S1A). In our dataset, we report global DNA methylation of ~65.5 %, which is lower than earlier WGBS datasets (~75.6% in (Guo et al., 2014) and 67.4-72.4% (Molaro et al., 2011)) (Figure 1G). This is suspected to arise from the selection of regions that are present during the PBAT sc-BS-seq protocol, as CpG site comparisons showed similar results. Overall, our analysis suggests that our sequencing data are of a comparative quality to similar published data.

Because of the high concordance between the results of our study cohort and the results obtained by Zhu et al., we included these data on 23 sperm cells in subsequent analyses to increase power. The

106 single-cell data from Zhu et al. all originated from the same individual and have not been
107 thoroughly used to investigate the role of DNA methylation in single-cell sperm.
108
109 **Autosomal differences in DNA methylation in X- and Y-carrying spermatozoa**
110 Given the plethora of sex-specific F1 phenotypes that have been reported in intergenerational
111 inheritance studies (Barbosa et al., 2016; Ng et al., 2010), we sought to determine if X-carrying
112 spermatozoa harbor distinct DNA methylation patterns compared to Y-carrying spermatozoa. “Sex”
113 of the spermatozoa was inferred by mapping reads to X and Y chromosomes (Figure 2A and Table
114 S1). Similar to bulk sequencing, X chromosomes carried more methylation than Y chromosomes
115 (Figure 2B). The autosomal chromosomes of X- and Y-carrying cells showed similar global DNA
116 methylation profiles (Figure 2C and Figure S2A). To further determine the association between the
117 presence of X or Y chromosomes on autosomal chromosome DNA methylation, we plotted the
118 spermatozoa autosomal DNA methylation signature of each sub-population on an MDS plot. We
119 found no clear separation of samples by sex chromosomes (Figure 2D). Analysis of DNA
120 methylation of autosomal chromosomes showed no difference in X- and Y-carrying spermatozoa
121 (Figure 2E). A similar result was observed when plotting DNA methylation of X vs. Y
122 chromosomes on a scatter plot, although this analysis revealed small potential differences (Figure
123 S2A). To further compare DNA methylation in X- and Y-carrying spermatozoa at higher resolution,
124 we performed a comparison at specific genomic regions: 1) gene promoters, 2) Coding Sequences
125 (CDS), and 3) at CpG dense regions, defined as stretches where CpGs are clustered with no more
126 than 100 base pairs apart (Table S2). We found two promoters with higher methylation in the male
127 spermatozoa, one for Tubulin Polyglutamylase Complex Subunit 1 (*TPGS1*) and one for Zic Family
128 Member 2 (*ZIC2*). No differential methylation was detected for CDS or CpG dense regions (Figure
129 S2B and Figure S2C). Overall, our results indicate that DNA methylation of autosomal

chromosomes is distinct in X- and Y-carrying spermatozoa, although these differences appear to be modest.

Extensive imprinting defects exist in subpopulations of spermatozoa within one ejaculate

Next, we examined DNA methylation patterns at imprinted genes in single spermatozoa. While we confirmed that, at the single cell level, maternally (*PEG3*) and paternally (*H19*) methylated imprinted genes had the expected DNA methylation patterns as bulk sequencing would predict (Figure S2A and Figure S2B), we detected two types of single cell imprinting defects. The first type is where a single CpG site was abnormally methylated, for example, at the Insulin-Like Growth Factor 2 (*IGF2*) locus (1,391 base stretch) (Figure 3A). The second type is where single cells carry extensive stretches of DNA methylation defects, with neighboring CpGs carrying similar hypo- or hypermethylation, as seen at the imprinted region near the Insulin-Like Growth Factor 2 Receptor (*IGF2R*) locus (1,002 base stretch) (Figure 3B). As we observed specific sperm cells carrying imprinting defects at long extensive stretches, we wondered if these cells might carry imprinting defects in other regions (Figure 3C). We found that extensive imprinting defects were mainly present at only one imprinted region or with only modest imprinting defects (< 50% DNA methylation change of the CpGs in the imprinted region), however, a minority of cells carried extensive defects at several regions. For example, one cell from the "Obese 4" participant had aberrant hypermethylation at the maternally imprinted genes *IGF1R (1,045 base stretch)*, *GPR1-AS (2,477 base stretch)*, and *GNAS XL (2,557 base stretch)*, and one cell from the "Lean 3" participant had hypermethylation defects at maternally imprinted genes *CXORF56 (1,095 base stretch)*, *GRB10 (2,585 base stretch)*, and *MKRN3 (5,409 base stretch)* (Figure 3C). Thus, our data show that both local and more global alterations of DNA methylation patterns at imprinted regions exist in

153 spermatozoa within the same ejaculate and suggest that these imprinting defects are not caused by a
154 general imprinting failure and may thus constitute large epimutations.
155
156 **Detection of higher DNA methylation variance at specific transposable elements**
157 To identify genomic regions of DNA methylation heterogeneity in single spermatozoa, we clustered
158 cells based on their methylation at individual CpG sites covered in at least 60 single spermatozoa in
159 the analysis. We identified a total of 292 CpG sites and observed that for most CpG sites, the
160 methylation state was similar across all sperm cells, independently of the donor (Figure S4A).
161 However, we did observe that 183 CpG sites had variations in DNA methylation in at least one of
162 the sperm cells investigated (Figure 4A). Clustering of the cells did not reveal any specific
163 subgroups of spermatozoa. As we observed a range of CpG sites in spermatozoa from the data of
164 Zhu et al. (Zhu et al., 2018) that carried a distinct DNA methylation profile, we sought to
165 investigate whether the difference in DNA methylation observed between spermatozoa of the
166 different cohorts and detected epimutations could be caused by nearby SNPs (Zhu et al., 2018). We
167 found that some of the regions had nearby SNPs, but overall, these did not affect DNA methylation
168 at the detected proximal CpG sites (Figure S4B). Clustering sperm based on methylation levels of
169 CpG dense regions (1,861 clusters covered by a minimum of 60 cells) revealed a similar pattern to
170 that of individual CpG sites, supporting the finding that variations in sperm cells are uniformly
171 distributed (Figure S4C). To determine if specific genomic regions exhibit DNA methylation
172 heterogeneity, we measured the standard deviation of DNA methylation based on the mean
173 methylation level at each CpG region (Figure 4B). Whereas regions at near 0% or 100%
174 methylation displayed consistent low variation, regions with intermediate methylation (25%-75%)
175 contained regions with both low and high variation (Figure 4B). Specifically, for the intermediately
176 methylated regions of high variation, we found that they were more often located far away from the

177 transcription start site, corresponding to being relatively more present in distal intergenic regions
178 and introns, while less present in promoter regions (Figure 4C and Figure S4D). When investigating
179 regions with extensive DNA methylation variation, we found that *young* Alu transposable elements
180 exhibited a particularly high level of DNA methylation variation. Stratifying DNA methylation
181 carried by specific species of transposable elements, we found that single cell DNA methylation
182 variation was higher in *young* Alu elements as well as certain species of LINE-1 (L1) retroelements
183 and "short interspersed nuclear element, variable number of tandem repeats, and Alu composite"
184 (SVA) (Figure 4D, Figure S4E and Figure S4F). As sequencing depth and average DNA
185 methylation level could be responsible for the higher variation found in the younger transposable
186 regions, we investigated the number of sequencing counts for each type of Alu element (Figure
187 S4G). We found that the Alu with the lowest genomic abundance and therefore the lowest number
188 of counts showed the highest variation (Figure S4G). We found that even though Alu, AluJ, and
189 AluS elements had differential variation, their variation did not seem to be affected by their DNA
190 methylation level (Figure S4H). Comparably, Zhu et al. (Zhu et al., 2018) observed higher variation
191 of methylation at young transposable elements. Since young Alu elements are less abundant than
192 old Alu elements, we down-sampled the coverage of the old Alu elements to match that of the
193 young Alu elements (Figure S4I), which indicates that higher variation of *young* Alu transposable
194 elements is biologically true rather than an artifact of sequencing bias.
195
196 **Single-cell differences in DNA methylation between lean and obese individuals**
197 Previously, we found that spermatozoa from humans with obesity have distinct DNA methylation
198 profiles compared to those of lean men (Donkin et al., 2016). To determine if epigenetic differences
199 are carried by the entire population in a mosaic-like fashion or by a sub-set of spermatozoa, we
200 analyzed single-cell bisulfite data of spermatozoa from lean and obese individuals, with a mean

BMI of 23.6 kg/cm^2 (22.3 kg/cm^2 -27.2 kg/cm^2) and 36.8 kg/cm^2 (32.7 - 40.9 kg/cm^2), respectively (Table 1). Visualization of single-cell sequencing data comparing spermatozoa of lean and obese men using dimensional scaling revealed a separation of cells from obese individuals at principal component 6 vs. 2, suggesting modest changes (Figure 5A and Figure S5A). Due to the lack of overlap between individual CpG's across our single-cell data, we opted to investigate differences in DNA methylation at the feature level, specifically at gene promoters, CDS and CpG dense regions (Table S3). We identified two CDS and two CpG dense regions with significantly different DNA methylation levels between cells from lean and obese men; one CDS region on chromosome 7 near *ASZ1* and one on chromosome 14 near *ENTPD5*, as well as one CpG dense region on chromosome 2, related to *LINC01237*, and one on chromosome 17, located near *PPM1D* (Figure 5C, Figure 5D, Figure S5A and Figure S5B). The cluster analysis for *LINC01237* and *PPM1D* at a single-cell level revealed that even across large regions (2074 and 775 base stretch for *LINC01237* and *PPM1D*, respectively), the differences in DNA methylation that we observed are carried by single cells, in a similar way to what we observed for imprinted genes. (Donkin et al., 2016). Our results suggest that some DNA methylation differences between obese and lean men are carried by a subset of spermatozoa.

DISCUSSION

Here we analyzed single-cell genome-wide DNA methylation data from spermatozoa of single ejaculates from several lean and obese individuals. We identify that within the same ejaculate, spermatozoa carrying X chromosomes have specific DNA methylation profiles compared to those carrying Y chromosomes. We confirm that spermatozoa from lean and obese men display distinct DNA methylation signatures, and we identify that a subset of spermatozoa within one ejaculate carry DNA methylation differences across large regions. Additionally, a subset of spermatozoa from single ejaculates exhibits large imprinting defects independently of BMI. Our results showing distinct epigenetic sub-populations of spermatozoa within an ejaculate have important implications for reproductive biology and assisted reproduction techniques.

Our study demonstrates that PBAT scBS-seq can be used to sequence single-cell spermatozoa and that the DNA methylation patterns obtained with this method are in good agreement across laboratories. However, this sequencing requires very high depth due to the low mapping rate and can only provide insight on a small fraction of the genome, with about 1-5 % of the total amount of CpGs covered in each cell. The fact that we observed a lower global methylation level compared to bulk sequencing suggests that the methylated and more tightly packaged heterochromatin was sequenced at a lower rate (Molaro et al., 2011). One way of solving this issue in future studies could be to use statistical models to predict neighboring CpG methylation. This method has been successfully performed in other cell types where larger datasets are available (Souza et al., 2020). Alternatively, future developments will undoubtedly allow for increased mapping rates and information to be recovered from more CpG sites. For example, bisulfite free methylation methods may prove useful and due to less harsh treatment conditions of DNA, may both increase mapping

243 rate and reduce bias in single-cell sequencing. However, these methods are still undergoing
244 validation in bulk sequencing (Liu et al., 2019). Overall, our results suggest that scBS may be
245 reliably used to detect DNA methylation of single spermatozoa between individuals and even across
246 laboratories. Nonetheless, the method has disadvantages, especially its cost efficiency, which is
247 very low due to the low mapping rate compared to WGBS methods.

248 As males and females differ only at the genetic level by the sex chromosomes most sexual
249 dimorphisms are assumed to be driven by gene expression differences on autosomal genes (Lopes-
250 Ramos et al., 2020; Oliva et al., 2020; Wijchers and Festenstein, 2011). Single-cell DNA
251 methylation sequencing of spermatozoa allowed, for the first time, the ability to compare if X and Y
252 chromosome DNA methylation differences exist on autosomal chromosomes before conception.
253 We show evidence of altered DNA methylation at two promoter regions. Given that we only
254 analyzed a fraction of the genome, more DNA methylation differences between X and Y
255 chromosome-carrying spermatozoa are likely when studying the whole genome. Interestingly, one
256 of the regions that we identified as differentially methylated is near the gene, *TPGS1*, which has a
257 sex-specific expression pattern in the neonatal mouse cortex/hippocampus before sexual
258 differentiation (Armoskus et al., 2014). Sex-specific DNA methylation differences have been
259 reported in both cord blood and placentas of newborns, as well as in the blood of adults, where it
260 was also linked to an altered gene expression pattern (Gong et al., 2018; Lopes-Ramos et al., 2020;
261 Maschietto et al., 2017; Oliva et al., 2020; Singmann et al., 2015). Understanding autosomal
262 differences will be important for examining the underlying cause of the plethora of sex-specific F1
263 phenotypes that have been reported in intergenerational inheritance studies (Barbosa et al., 2016;
264 Ng et al., 2010).

265 There is a growing number of known imprinting disorders, which affect early embryonic
266 development, brain development, male infertility (Hajj et al., 2011; Hattori et al., 2019; Santi et al.,

2017) and metabolic adaption later in life (Constância et al., 2004; Tucci et al., 2019). Strikingly, we found that single spermatozoa within an ejaculate have extensive DNA methylation defects at several imprinted regions. This finding is interesting as it has been reported that some patients with imprinting disorders such as Beckwith-Wiedemann syndrome may have more generalized imprinting defects (Bliek et al., 2009; Eggermann et al., 2008). Moreover, imprinted regions are candidates for carrying epigenetic inheritance effects, as these regions escape epigenetic reprogramming after fertilization (Smallwood et al., 2011; Tang et al., 2015; Zhu et al., 2018). Thus, our data demonstrating that some spermatozoa have specific imprinting defects supports a mechanism by which environmentally induced erroneous reprogramming at imprinted regions may not be erased after fertilization. This mechanism may contribute to epigenetic effects in the next generation. It is essential to highlight that the ejaculates that we used in our study were subjected to a swim-up procedure. Therefore, all the spermatozoa that we studied, even those with imprinting defects, were motile and carried the potential to reach the egg. Given the possible dramatic influence of imprinting defects on the development of the embryo and the health of the offspring, our results open a new perspective when considering the selection of spermatozoa, for example, during intracytoplasmic sperm injection.

Our investigations revealed that DNA methylation is mostly homogeneous in spermatozoa, with most DNA methylation variability being equally distributed across the spermatozoa population in a mosaic-like fashion. However, few spermatozoa showed marked imprinting defects. Here, since we have analyzed motile spermatozoa from our swim-up extraction method, our results do not suggest that imprinting defects are carried solely by immotile spermatozoa. Intra-ejaculate differences in sperm DNA methylation have been reported between high-quality and low-quality spermatozoa purified *via* density gradient (Jenkins et al., 2015). An increased coefficient of DNA methylation variation was found in the low-quality subpopulation, and, interestingly, this variation

291 was rarely observed in the same locus between subjects, supporting the idea that the variability in
292 DNA methylation is spread in a random mosaic-like fashion (Jenkins et al., 2015). Our study did
293 find specific regions that presented with a higher variation in DNA methylation. Especially, our
294 finding that young Alu elements have higher variation is intriguing, as these particular regions are
295 associated with spermatozoa fertility potential and constitute one of the few regions that undergo *de*
296 *novo* methylation in the early developing zygote (Hajj et al., 2011; Zhu et al., 2018). Transposable
297 elements are key drivers of gene expression during early embryonic development, specifically
298 during zygotic gene activation (reviewed in Rodriguez-Terrones & Torres-Padilla
299 2018)(Rodriguez-Terrones and Torres-Padilla, 2018). In particular, young transposable elements
300 may play an important role in early paternal gene expression (Zhu et al., 2018). While we could not
301 rule out that the detection of increased variance at young Alu elements was not caused by a
302 sequencing bias, it is tempting to speculate that increased variance of young, compared to ancient,
303 Alu elements is due to less efficient DNA methylation maintenance at these regions, thereby
304 leading to phenotypic stochasticity in the next generation.

305 Obesity is associated with specific DNA methylation patterns in human spermatozoa when
306 sequenced in bulk. Here, we confirmed that at the single-cell level also, obesity is associated with
307 differential DNA methylation in sperm. However, the differentially methylated regions we
308 identified did not overlap with regions previously identified by our group (Donkin et al., 2016).
309 This is likely to be due to the difference in the areas covered as well as the method that we used in
310 the two analyses (Reduced Representation Bisulfite Sequencing of bulk (Donkin et al., 2016) and
311 PBAT scBS-seq (Clark et al., 2017)). Our data indicate that differences between groups may be
312 driven by large hypo- or hypermethylated regions in individual cells, similar to what was observed
313 in imprinted regions. Such single cell specific DNA methylation patterns at specific loci may be due
314 to the processive binding of enzymes establishing and removing DNA methylation (Rulands et al.,

2018). It is possible that few cells carry most or all the aberrant methylation patterns, however, the limited coverage inherent to single-cell sequencing did not allow us to determine if the same cells carry aberrant methylation profiles at more than one locus.

Our results allow us to model the mechanisms of epigenetic inheritance, which may involve sperm DNA methylation. In intergenerational epigenetic studies, most of the reported changes in sperm DNA methylation are within the 5-15 % difference range at specific sites (Donkin and Barrès, 2018). In haploid cells like spermatozoa, such figures imply that 5 to 15 spermatozoa out of 100 would have an altered DNA methylation pattern for this specific CpG. Yet, offspring phenotypes described in paternal effects show high penetrance, suggesting that DNA methylation changes driving the phenotypic response may occur at distinct CpG sites, which would independently affect the offspring towards the same phenotype. Given the extensive mosaicism in DNA methylation patterns that we found in spermatozoa within an ejaculate, this mechanism would require that different patterns of CpG methylation variation are integrated into one single phenotype. Such model, by which methylation variation at different genes leads to an integrated phenotypic alteration is plausible in the case of metabolic dysfunction, a phenotype very often measured in epigenetic inheritance studies, as metabolic disorders like obesity and type 2 diabetes are polygenic (Flannick and Florez, 2016; Kong et al., 2012; Manolio et al., 2009; Morris et al., 2012).

From animal studies, it is clear that DNA methylation is essential for spermatogenesis and sperm maturation, as shown by knock-out models of DNA methyltransferases and treatment of animals with the hypomethylation agent 5-azacytidine (Oakes et al., 2007; Takashima et al., 2009; Vasiliauskaitė et al., 2018). Besides a decreased ability to develop mature spermatozoa, one study showed a reduced capacity of the developed spermatozoa, with altered DNA methylation, to reach the blastocyst stage of embryo development (Vasiliauskaitė et al., 2018). In humans, DNA

339 methylation predicts embryo quality (Aston et al., 2015; Jenkins et al., 2016). Correspondingly a
340 link between DNA methylation patterns in sperm and reproductive capacity has been established in
341 obese men, where survival at the cleavage stage (2-cell stage) was equal to fertile controls,
342 however, after genome activation (blastocyst stage), survival was significantly decreased in
343 embryos fertilized by sperm from obese men (Bakos et al., 2011). In light of the elevated risk of
344 developing imprinting disorders in offspring born from assisted reproduction (Hattori et al., 2019;
345 Henningsen et al., 2020; Johnson et al., 2018; Uk et al., 2018), our results suggest that the
346 subpopulation of spermatozoa carrying imprinting defects may be positively selected by assisted
347 reproduction techniques. Our results provide a substantial addition to our understanding of the
348 mechanisms driving epigenetic inheritance and potentially pave the way for the development of
349 novel assisted reproduction strategies aiming to ensure health in the next generation.
350
351

METHODS

Sample collection:

Single ejaculate semen samples were collected from five lean (BMI 20-25) and five obese (BMI 30-45) male subjects in the age range of 20-36 years. Exclusion criteria were daily intake of prescription medicine, smoking, and testicular disease. All participants were controlled for testicular abnormalities by anamnesis. Sperm ejaculates were delivered after 3-5 days of abstinence and stored at 37°C for 30 minutes for liquefaction of the samples. Basic semen parameters, including volume, concentration, and motility were inspected by manual counting on a phase contrast microscope according to WHO guidelines (WHO, 2010) at room temperature (22°C). The human study was approved by the regional ethical committee for the Capital Region of Denmark (Videnskabsetisk Komité, Kongens Vænge 2, 3400 Hillerød, Denmark, Journal no. H-17041722). All participants provided written informed consent before participating in the study.

Isolation of motile spermatozoa

A swim-up procedure was performed to isolate motile spermatozoa from non-motile spermatozoa and somatic cells. Before this, volume of ejaculates was determined by wide-bore volumetric pipetting. As previously described (Donkin et al., 2016), 0.5 ml of semen was overlaid with 2 ml of swim-up media, comprising of Earle's Balanced Salt Solution (Sigma-Aldrich, Germany) with 3.2 mg/ml Human Serum Albumin (Sigma-Aldrich, Germany) and 25 mM Hepes (Sigma-Aldrich, Germany) in round-bottom tubes and incubated for 2 hours at 37°C with 5% CO2 at a 45° angle (Donkin et al., 2016). The upper fractions were pooled per ejaculate, centrifuged, resuspended in Phosphate-Buffered Saline (ThermoFisher) and the spermatozoa counted while presence of somatic cells was inspected and noted.

376

377 *Single cell sorting*

378 Single spermatozoa were collected by flow cytometry directly into a well of a 96 well plate,
379 containing 5 µl RLT plus (Qiagen) with 1% v/v β-mercaptoethanol (Biorad), using a BD
380 FACSAria™ III. Before sorting, Hoechst 33258 (Sigma) was used to label the DNA content of the
381 cells as previously described (Smallwood et al., 2014a). Briefly, Hoechst were added to the
382 resuspended motile sperm cells, in a concentration of 5 µg/ml for 10 minutes. After staining, the
383 sperm were washed 2 times before flow cytometry. The sperm cells were stored at -80°C until
384 required for library preparation. Negative controls were lysis buffer alone and were prepared and
385 processed in parallel with single-cell samples.

386

387 *Single-cell library preparation*

388 Collected cells were thawed and the following solution was added: 1 µl 10% SDS, 1 µl 0.1M DTT,
389 2 µl Proteinase K (800 units/µl, Sigma), 0.01µl 1M $CaCl_2$ and 0.99µl H_20. The cells were then
390 incubated for 6 hours at 50 °C for complete lysis. Bisulfite conversion was performed on cell
391 lysates using the EZ DNA Methylation-Direct kit (Zymo). Compared to our original protocol, we
392 modified the conversion to include an extra 98 °C heating for 3 min, 38 min into the conversion
393 step (Clark et al., 2017): i.e. incubation was 98C 8min, 64C 30min, 98C 3min, 64C 3 hours.
394 Purification was performed as previously described (Clark et al., 2017), and DNA was eluted
395 directly into 39ul of first strand synthesis master mix: 0.4 mM dNTPs, 0.4 µM oligo 1 (a truncated
396 Illumina read 1 sequence followed by six random bases) and 1× Blue Buffer (Enzymatics) before
397 incubation at 65 °C for 3 min followed by a 4 °C pause. 50 U of Klenow exo– (Enzymatics) was
398 added and the samples were incubated at 4 °C for 5 min, +1 °C/15 s to 37 °C, 37 °C for 30 min.
399 Samples were incubated at 95 °C for 1 min and transferred immediately to ice before addition of

fresh oligo 1 (10 pmol), Klenow exo– (25 U), and dNTPs (1 nmol) in 2.5 µl of 1x blue buffer. The samples were incubated at 4 °C for 5 min, +1 °C/15 s to 37 °C, 37 °C for 30 min. This random priming and extension was repeated a further three times (five rounds in total). Samples were then incubated with 40 U exonuclease I (NEB) for 1 h at 37 °C before DNA was purified using 0.8× Agencourt Ampure XP beads (Beckman Coulter) according to the manufacturer's guidelines. Samples were eluted in 49 µl of 0.4 mM dNTPs, 0.4 µM oligo 2 and 1× Blue Buffer. Samples were incubated at 95 °C for 45 s and transferred immediately to ice before addition of 50 U Klenow exo– (Enzymatics) and incubation at 4 °C for 5 min, +1 °C/15 s to 37 °C, 37 °C for 90 min. Samples were purified with the addition of 50ul of water and 80ul of binding buffer (Agencourt Ampure XP beads with the beads removed). After two ethanol washes, beads were resuspended in 50 µl of 0.4 mM dNTPs, 0.4 µM PE1.0 forward primer, 0.4 µM indexed iPCRTag reverse primer, 1 U KAPA HiFi HotStart DNA Polymerase (KAPA Biosystems) in 1× HiFi Fidelity Buffer. Libraries were then amplified by PCR as follows: 95 °C 2 min, 14 repeats of (94 °C 80 s, 65 °C 30 s, 72 °C 30 s), 72 °C 3 min and 4 °C hold. Amplified libraries were purified using 0.8× Agencourt Ampure XP beads, according to the manufacturer's guidelines, and were assessed for quality and quantity using High-Sensitivity DNA chips on the Agilent Bioanalyzer, and the KAPA Library Quantification Kit for Illumina (KAPA Biosystems). Pools of 12–14 single cell libraries were prepared for 100-bp paired-end sequencing on a HiSeq2500 in rapid-run mode (2 lanes/run).

Bioinformatics:

Reads were pre-processed by Trim Galore v. 0.5.0_dev. Alignment, deduplication, and summarization was performed by Bismark v. 0.20.0 with the --non_directional flag set. Forward and reverse reads were processed separately. Further processing was performed using R and figures were generated using ggplot2. Coverage files generated by Bismark was imported into R.

Chromosome M was excluded and CpGs were filtered to only include CpGs covered by a single fragment, not hemi-methylated and a CpG in hg38 reference genome. Forward and reverse reads were aggregated to cell level methylation. In cases where a CpG was covered by both the forward and reverse read, the forward read methylation status was used. CpGs overlapping NCBI dbSNP Build 151 (Sherry et al., 2001) were excluded. Each CpG overlapping a promoter or a CDS was annotated with the gene ID and each CpG was overlapped with a CpG cluster, where a cluster is defined as a stretch of DNA with no more than 100 bp between CpG's. Cells were annotated as X carrying if there was more than 10 times more reads on the X chromosome than on the Y, and Y carrying the opposite. Data from Zhu et al. (Zhu et al., 2018) was processed in a similar manner, except the processing started at Bismark coverage files. Prior to testing for differential methylation, all cells from the same individual were summed up to create a pseudo-bulk dataset. Differential methylation was tested using edgeR. Differential methylation was tested on CpGs aggregated onto clusters, promoters and CDSs. Only regions with eight or more observations were tested. Heatmap figures comparing our data and the data from Zhu et al. (Zhu et al., 2018) as well as the X vs Y carrying spermatozoa was performed based on averages per cluster. Imprinted region was obtained from (Court et al., 2014) and lifted to hg38 using liftOver, additional regions was obtained from (Fend-Guella et al., 2019). Multidimensional scaling (MDS) plots was generated in two steps, first pairwise distances between all samples were calculated as one minus the simple matching coefficient of the methylation status of CpG cites covered in both samples, next principal component analysis was performed on the distance matrix. For the comparisons between autosomal chromosome DNA methylation for X and Y carrying spermatozoa, all covered CpG's were used and tested using the Kolmogorov–Smirnov test. Genomic annotations of promoters, introns and exons was obtained from GENCODE v. 31 (Frankish et al., 2018), CpG islands and transposable elements was obtained from the UCSC Table Browser (Karolchik et al., 2004) and piRNAs were

448 obtained from piRNAdb (www.pirnadb.org). CpG sites were considered near a mutation if the read
449 they originated from contained a mismatch relative to the hg38 reference genome.

450 *Data and code availability:*

451 Datasets were deposited in the Gene Expression Omnibus (GEO), with the following GEO
452 accession numbers (GSEXXXX). Single-cell analysis pipeline is accessible at: Github

453

454 **STAR METHODS**

REAGENT or RESOURCE	SOURCE	IDENTIFIER
Antibodies		
Hoechst 33342	Sigma	Cat# 14533-100MG
Chemicals, Peptides and Recombinant proteins		
Earle's Balanced Salt Solution	Sigma	Cat# E2888
Human Serum Albumin	Sigma	Cat# A5843
Hepes	Sigma	Cat# H3375
Phosphate-buffered saline	ThermoFisher	Cat# 20012068
RLT plus	Qiagen	Cat# 1053393
Beta-mercaptoethanol	Biorad	Cat# 161-0710
1M Tris-HCl, pH 8.0	Gibco	Cat# 15568-025
0.5M EDTA solution	Sigma	Cat# E7889-100ML
5M NaCl	Sigma	Cat# 71386
Tween-20	Sigma	Cat# P9416
Poly (ethylene glycol) 8000	Sigma	Cat# 89510
Unmethylated Lambda DNA	Promega	Cat# D152A
dNTPs	Roche	Cat# 11969064001
Critical Commercial Assays		
Agencourt AMPure XP beads	Beckman Coulter	Cat# 63881
Klenow (3'-5' Exo) High Concentration	Enzymatics	Cat# P7010-HC-L
Exonuclease I	NEB	Cat# M0293L
KAPA HiFi HotStart DNA polymerase	KAPA Biosystems	Cat# KK2502
KAPA HiFi Fidelity Buffer, supplied with polymerase	KAPA Biosystems	Cat# KK2502
KAPA Illumina library quantification kit	KAPA Biosystems	Cat# KK4824

Agilent high-sensitivity DNA kit	Agilent Technologies	Cat# 5067-4626
Zymo EZ Methylation Direct MagPrep kit	Zymo	Cat# D5044
Deposited Data		
Raw sequence data and count tables	This study	GEO XXX
Single-cell DNA methylome sequencing	Zhu et al 2018	GSE81233
Single-cell multi-omics sequencing	Li et al 2019	GSE100272
Oligonucleotides		
Preamp Oligo	(Clark et al., 2017)	
CTACACGACGCTCTTCCGATCTNNNNNN		
Adapter 2 Oligo	(Clark et al., 2017)	
TGCTGAACCGCTCTTCCGATCTNNNNNN		
PE1.0	(Clark et al., 2017)	
AATGATACGGCGACCACCGAGATCTACACTCTTTCCCTACACGACGCTCTTCCGATC*T		
iPCRTag	(Clark et al., 2017)	
CAAGCAGAAGACGGCATACGAGATNNNNNNNNGAGATCGGTCTCGGCATTCCTGCTGAACCGCTCTTC CGATC*T		
iTag sequencing primer	(Clark et al., 2017)	
AAGAGCGGTTCAGCAGGAATGCCGAGACCGATCTC		
Software and Algorithms		
FastQC	http://www.bioinformatics.babraham.ac.uk/projects/fastqc/	
Trim Galore	www.bioinformatics.babraham.ac.uk/projects/trim_galore/	
Cutadapt34	https://cutadapt.readthedocs.org/en/stable/	
Bismark35	http://www.bioinformatics.babraham.ac.uk/projects/bismark/)	
Bowtie236	http://bowtie-bio.sourceforge.net/bowtie2/index.shtml	
Ggplot2	https://ggplot2.tidyverse.org	
R	https://www.R-project.org/.	
edgeR	https://bioconductor.org/packages/release/bioc/html/edgeR.html	
liftOver	https://bioconductor.org/packages/release/workflows/html/liftOver.ht	

ml

455

456

DECLARATION OF INTERESTS

W.R. is a consultant and shareholder of Cambridge Epigenetix. E.A. is employed and a shareholder of ExSeed Health ApS. The other authors declare no competing interests.

ACKNOWLEDGMENTS

The authors would like to acknowledge the Flow Cytometry Platform, at the Novo Nordisk Foundation Center for Stem Biology (DanStem) and Center for Protein Research (CPR) for their support and technical expertise. We thank the members of the Barrès Group for their critical reading of the manuscript and helpful comments. The Novo Nordisk Foundation Center for Basic Metabolic Research (http://www.metabol.ku.dk) is an independent research Center at the University of Copenhagen, partially funded by an unrestricted donation from the Novo Nordisk Foundation.

AUTHOR CONTRIBUTIONS

R.B. and W.R. designed the experiments. E.A. carried out sample collection, swim-up procedure, and flow cytometry isolation. S.C. and E.A. carried out PBAT scBS-seq library preparation. L.R.I performed single cell computational analysis. All authors carried out data analysis and wrote the manuscript.

476 **FIGURE LEGENDS**

477

478 **Figure 1. Benchmark of DNA methylation results from single cell spermatozoa**

479 (A) Schema describing the PBAT scBS-seq method and study participants. Blue and red represents
480 lean and obese respectively.

481 (B) Number of spermatozoa analyzed in each group and based on sex chromosome. All
482 spermatozoa were isolated from the semen sample with a swim-up method to isolate motile
483 spermatozoa and then sorted into a 96-well via flow cytometry using Hoechst 33258 to stain for
484 DNA.

485 (C) Number of CpGs covered by scBS-seq as a function of total mapped sequences compared to a
486 reference dataset (Zhu et al., 2018).

487 (D) DNA methylation levels comparing spermatozoa from our cohort with spermatozoa from Zhu
488 et al. (Zhu et al., 2018).

489 (E) DNA methylation level comparing spermatozoa from our cohort with oocytes from Zhu et al
490 (Zhu et al., 2018).

491 (F) MDS analysis of the DNA methylation profile of single cells compared to spermatozoa and
492 oocytes from Zhu et al (Zhu et al., 2018), with the removal of four outliers described in Zhu et al
493 (Zhu et al., 2018).

494 (G) Average DNA methylation of single spermatozoa based on region and subject.

495

Figure 2. Distinct DNA methylation landscape in sperm with X and Y chromosome

(A) Schema of X and Y chromosome carrying spermatozoa. Green and orange denotes X chromosome carrying and Y chromosome carrying spermatozoa.

(B) Global DNA methylation level of the X and Y chromosome single spermatozoa.

(C) Global DNA methylation of autosomal chromosomes in X and Y chromosome single spermatozoa.

(D) MDS analysis of the DNA methylation profile of single cells based on sex chromosomes.

(E) Bean plot of autosomal DNA methylation based on chromosome and sex chromosome. Kolmogorov–Smirnov test showed no difference in chromosome DNA methylation of X and Y carrying spermatozoa.

507 **Figure 3. Single spermatozoa carry imprinting DNA methylation defects**

508 (A) DNA methylation of single spermatozoa at the imprinted region *IGF2*.

509 (B) DNA methylation of single spermatozoa at the imprinted region *IGF2R*.

510 (C) Heat map of the DNA methylation patterns at imprinting regions in single spermatozoa.

511

512 **Figure 4. Heterogeneity of DNA methylation at transposable regions in single spermatozoa**

513 (A) Plotting of the DNA methylation levels at single CpG sites found in at least 60 single
514 spermatozoa and where a variable DNA methylation was found in at least one single spermatozoa.
515 Each line represents a single cell, and each dot represents a given CpG. The location of the CpGs is
516 spread across the genome.

517 (B) DNA methylation variation in single cell DNA methylation clustered by region.

518 (C) Location of stable and variable DNA methylation clusters based on genomic regions.

519 (D) Single cell DNA methylation level at repetitive elements. Each dot represents the DNA
520 methylation level in a specific single cell.

521

522 **Figure 5. Differential methylation of single spermatozoa in lean *vs.* obese**

523 (A) MDS analysis of DNA methylation profiles of single cells from lean and obese individuals.

524 (B) DNA methylation of the region *LINC01237* in single spermatozoa from the various participants.

525 (C) DNA methylation of the region *PPM1D* in single spermatozoa from the various participants.

526

SUPPLEMENTARY FIGURE LEGENDS

Figure S1. MDS analysis of the DNA methylation profile of single spermatozoa of our cohort compared to spermatozoa and oocytes from Zhu et al.

Figure S2. Global and regional DNA methylation differences between X and Y-chromosome carrying spermatozoa

(A) DNA methylation levels of X chromosome compared to Y chromosome.

(B) DNA methylation of the differentially methylated *TPGS1* region distributed by X- and Y-carrying chromosomes.

(C) Single spermatozoa DNA methylation of the differentially methylated ZIC2 region distributed by X and Y carrying chromosomes in single cells of subjects.

Figure S3. Single spermatozoa DNA methylation at control imprinted regions.

(A) Single spermatozoa DNA methylation of the maternally imprinted region PEG3.

(B) Single spermatozoa DNA methylation of the paternally imprinted region H19.

Figure S4. Single-cell DNA methylation heterogeneity of spermatozoa at transposable regions of younger origin.

(A) DNA methylation at single CpG sites found in at least 60 single spermatozoa. Each line represents a single spermatozoon, and each dot represents a given CpG. The location of the CpGs is spread across the genome.

(B) DNA methylation at single CpG sites found in at least 60 single cells, with a variable DNA methylation in at least one single spermatozoa. Each line represents a single cell, and each dot

551 represents a given CpG. Each dot is colored by DNA methylation state; green (unmethylated) / blue
552 (methylated), and if a SNP was identified within 100 base pairs of the given CpG, light (SNP
553 nearby) / dark (no SNP nearby). The location of the CpGs is spread across the genome.
554 (C) DNA methylation at CpG dense regions identified in all at least 60 single spermatozoa. Each
555 line represents a single cell, and each dot represents a given methylation state of a CpG cluster. The
556 location of the CpG dense regions is spread across the genome.
557 (D) Location of stable and variable DNA methylation clusters based on distance to transcription
558 start site (TSS).
559 (E) Single cell DNA methylation level at repetitive elements. Each dot represents the DNA
560 methylation level in a specific single spermatozoa.
561 (F) Single cell DNA methylation level at repetitive elements. Each dot represents the DNA
562 methylation level in a specific single spermatozoa.
563 (G) DNA methylation variance of Alu subclasses based on their genomic frequency.
564 (H) Mean DNA methylation of Alu subclasses based on their genomic frequency.
565 (I) Single cell DNA methylation level of Alu subclasses where the coverage of each subclass has
566 been down sampled to match that of the lowest Alu subclass per each participant. Each dot
567 represents the DNA methylation level at specific single spermatozoa.
568
569 **Figure S5. Differentially methylated regions of single-cell spermatozoa from lean and obese**
570 **individuals.**
571 (A) Single spermatozoa DNA methylation of the region *ASZ1* distributed in subjects.
572 (B) Single spermatozoa DNA methylation of the region *ENTPD5* distributed in subjects.
573

TABLES

Table 1. Clinical characteristics of subjects

	Lean (n = 4)	Obese (n=4)
Age (yr)	24.25 [21-26]	32.21 [23.13-47.17]
Weight (kg)	82.25 [69-98]	120.2 [97.4-142.7]*
Height (m)	1.86 [1.76-1.93]	1.80 [1.73-1.93]
BMI (kg/m^2)	23.62 [22.26-27.15]	36.79 [32.66-40.91]*
Volume (ml)	3.16 [0.95-5.3]	2.33 [1.45-2.7]
Sperm concentration (million/ml)	88.50 [20.40-115.60]	53.06 [6.10-122.70]
Total sperm count (million)	328.68 [19.38-604.20]	140.04 [8.85-331.29]
Motile (%)	36.82 [8.6-62.42]	26.87 [17.9-41.01]
Total motile sperm count (million)	136.16 [5.28-377.14]	37.66 [2.43 - 69.90]

Data are represented as mean (minimum-maximum).

*Difference versus lean analyzed with student's t-test.

SUPPLEMENTARY TABLES:

Table S1. Sequencing statistics

Table S2. X vs Y chromosome differentially methylated regions

Table S3. Differentially methylated regions between lean and obese

587 **REFERENCES**

588

589 Armoskus, C., Moreira, D., Bollinger, K., Jimenez, O., Taniguchi, S., and Tsai, H.-W. (2014).
590 Identification of sexually dimorphic genes in the neonatal mouse cortex and hippocampus. Brain
591 Res *1562*, 23–38.

592 Aston, K.I., Uren, P.J., Jenkins, T.G., Horsager, A., Cairns, B.R., Smith, A.D., and Carrell, D.T.
593 (2015). Aberrant sperm DNA methylation predicts male fertility status and embryo quality. Fertil
594 Steril *104*, 1388-1397.e5.

595 Bakos, H.W., Henshaw, R.C., Mitchell, M., and Lane, M. (2011). Paternal body mass index is
596 associated with decreased blastocyst development and reduced live birth rates following assisted
597 reproductive technology. Fertil Steril *95*, 1700–1704.

598 Barbosa, T. de C., Ingerslev, L.R., Alm, P.S., Versteyhe, S., Massart, J., Rasmussen, M., Donkin, I.,
599 Sjögren, R., Mudry, J.M., Vetterli, L., et al. (2016). High-fat diet reprograms the epigenome of rat
600 spermatozoa and transgenerationally affects metabolism of the offspring. Mol Metab *5*, 184–197.

601 Bliek, J., Verde, G., Callaway, J., Maas, S.M., Crescenzo, A.D., Sparago, A., Cerrato, F., Russo, S.,
602 Ferraiuolo, S., Rinaldi, M.M., et al. (2009). Hypomethylation at multiple maternally methylated
603 imprinted regions including PLAGL1 and GNAS loci in Beckwith–Wiedemann syndrome. Eur J
604 Hum Genet *17*, 611–619.

605 Clark, S.J., Smallwood, S.A., Lee, H.J., Krueger, F., Reik, W., and Kelsey, G. (2017). Genome-
606 wide base-resolution mapping of DNA methylation in single cells using single-cell bisulfite
607 sequencing (scBS-seq). Nat Protoc *12*, 534–547.

608 Conine, C.C., Sun, F., Song, L., Rivera-Pérez, J.A., and Rando, O.J. (2018). Small RNAs Gained
609 during Epididymal Transit of Sperm Are Essential for Embryonic Development in Mice. Dev Cell
610 *46*, 470-480.e3.

611 Constância, M., Kelsey, G., and Reik, W. (2004). Resourceful imprinting. Nature *432*, 53–57.

612 Court, F., Tayama, C., Romanelli, V., Martin-Trujillo, A., Iglesias-Platas, I., Okamura, K.,
613 Sugahara, N., Simón, C., Moore, H., Harness, J.V., et al. (2014). Genome-wide parent-of-origin
614 DNA methylation analysis reveals the intricacies of human imprinting and suggests a germline
615 methylation-independent mechanism of establishment. Genome Res *24*, 554–569.

616 Denham, J., O'Brien, B.J., Harvey, J.T., and Charchar, F.J. (2015). Genome-wide sperm DNA
617 methylation changes after 3 months of exercise training in humans. Epigenomics-Uk *7*, 717–731.

618 Donkin, I., and Barrès, R. (2018). Sperm epigenetics and influence of environmental factors. Mol
619 Metab *14*, 1–11.

620 Donkin, I., Versteyhe, S., Ingerslev, L.R., Qian, K., Mechta, M., Nordkap, L., Mortensen, B.,
621 Appel, E.V.R., Jørgensen, N., Kristiansen, V.B., et al. (2016). Obesity and Bariatric Surgery Drive
622 Epigenetic Variation of Spermatozoa in Humans. Cell Metab *23*, 369–378.

623 Eggermann, T., Eggermann, K., and Schönherr, N. (2008). Growth retardation versus overgrowth:
624 Silver-Russell syndrome is genetically opposite to Beckwith-Wiedemann syndrome. Trends Genet
625 *24*, 195–204.

626 Fend-Guella, D.L., Kopylow, K. von, Spiess, A.-N., Schulze, W., Salzbrunn, A., Diederich, S.,
627 Hajj, N.E., Haaf, T., Zechner, U., and Linke, M. (2019). The DNA methylation profile of human
628 spermatogonia at single-cell- and single-allele-resolution refutes its role in spermatogonial stem cell
629 function and germ cell differentiation. Mol Hum Reprod *25*, 283–294.

630 Flannick, J., and Florez, J.C. (2016). Type 2 diabetes: genetic data sharing to advance complex
631 disease research. Nat Rev Genet *17*, 535–549.

632 Frankish, A., Diekhans, M., Ferreira, A.-M., Johnson, R., Jungreis, I., Loveland, J., Mudge, J.M.,
633 Sisu, C., Wright, J., Armstrong, J., et al. (2018). GENCODE reference annotation for the human
634 and mouse genomes. Nucleic Acids Res *47*, gky955-.

635 Gong, S., Johnson, M.D., Dopierala, J., Gaccioli, F., Sovio, U., Constância, M., Smith, G.C., and
636 Charnock-Jones, D.S. (2018). Genome-wide oxidative bisulfite sequencing identifies sex-specific
637 methylation differences in the human placenta. Epigenetics *13*, 01–32.

638 Guo, H., Zhu, P., Yan, L., Li, R., Hu, B., Lian, Y., Yan, J., Ren, X., Lin, S., Li, J., et al. (2014). The
639 DNA methylation landscape of human early embryos. Nature *511*, 606–610.

640 Guo, H., Zhu, P., Guo, F., Li, X., Wu, X., Fan, X., Wen, L., and Tang, F. (2015). Profiling DNA
641 methylome landscapes of mammalian cells with single-cell reduced-representation bisulfite
642 sequencing. Nat Protoc *10*, 645–659.

643 Hajj, N.E., Zechner, U., Schneider, E., Tresch, A., Gromoll, J., Hahn, T., Schorsch, M., and Haaf,
644 T. (2011). Methylation Status of Imprinted Genes and Repetitive Elements in Sperm DNA from
645 Infertile Males. Sex Dev *5*, 60–69.

646 Hammoud, S.S., Nix, D.A., Zhang, H., Purwar, J., Carrell, D.T., and Cairns, B.R. (2009).
647 Distinctive chromatin in human sperm packages genes for embryo development. Nature *460*, 473–
648 478.

649 Hattori, H., Hiura, H., Kitamura, A., Miyauchi, N., Kobayashi, N., Takahashi, S., Okae, H., Kyono,
650 K., Kagami, M., Ogata, T., et al. (2019). Association of four imprinting disorders and ART. Clin
651 Epigenetics *11*, 21.

652 Henningsen, A.A., Gissler, M., Rasmussen, S., Opdahl, S., Wennerholm, U.B., Spangsmose, A.L.,
653 Tiitinen, A., Bergh, C., Romundstad, L.B., Laivuori, H., et al. (2020). Imprinting disorders in
654 children born after ART: a Nordic study from the CoNARTaS group. Hum Reprod *35*, 1178–1184.

655 Ingerslev, L.R., Donkin, I., Fabre, O., Versteyhe, S., Mechta, M., Pattamaprapanont, P., Mortensen,
656 B., Krarup, N.T., and Barrès, R. (2018). Endurance training remodels sperm-borne small RNA
657 expression and methylation at neurological gene hotspots. Clin Epigenetics *10*, 12.

658 Jenkins, T.G., Aston, K.I., Trost, C., Farley, J., Hotaling, J.M., and Carrell, D.T. (2015). Intra-
659 sample heterogeneity of sperm DNA methylation. Mhr Basic Sci Reproductive Medicine *21*, 313–
660 319.

661 Jenkins, T.G., Aston, K.I., Meyer, T.D., Hotaling, J.M., Shamsi, M.B., Johnstone, E.B., Cox, K.J.,
662 Stanford, J.B., Porucznik, C.A., and Carrell, D.T. (2016). Decreased fecundity and sperm DNA
663 methylation patterns. Fertil Steril *105*, 51-57.e3.

664 Johnson, J.P., Beischel, L., Schwanke, C., Styren, K., Crunk, A., Schoof, J., and Elias, A.F. (2018).
665 Overrepresentation of pregnancies conceived by artificial reproductive technology in prenatally
666 identified fetuses with Beckwith-Wiedemann syndrome. J Assist Reprod Gen *35*, 985–992.

667 Kaneda, M., Okano, M., Hata, K., Sado, T., Tsujimoto, N., Li, E., and Sasaki, H. (2004). Essential
668 role for de novo DNA methyltransferase Dnmt3a in paternal and maternal imprinting. Nature *429*,
669 900–903.

670 Karolchik, D., Hinrichs, A.S., Furey, T.S., Roskin, K.M., Sugnet, C.W., Haussler, D., and Kent,
671 W.J. (2004). The UCSC Table Browser data retrieval tool. Nucleic Acids Res *32*, D493–D496.

672 Kong, A., Frigge, M.L., Masson, G., Besenbacher, S., Sulem, P., Magnusson, G., Gudjonsson, S.A.,
673 Sigurdsson, A., Jonasdottir, A., Jonasdottir, A., et al. (2012). Rate of de novo mutations and the
674 importance of father's age to disease risk. Nature *488*, 471–475.

675 Liu, Y., Siejka-Zielińska, P., Velikova, G., Bi, Y., Yuan, F., Tomkova, M., Bai, C., Chen, L.,
676 Schuster-Böckler, B., and Song, C.-X. (2019). Bisulfite-free direct detection of 5-methylcytosine
677 and 5-hydroxymethylcytosine at base resolution. Nat Biotechnol *37*, 424–429.

678 Lopes-Ramos, C.M., Chen, C.-Y., Kuijjer, M.L., Paulson, J.N., Sonawane, A.R., Fagny, M., Platig,
679 J., Glass, K., Quackenbush, J., and DeMeo, D.L. (2020). Sex Differences in Gene Expression and
680 Regulatory Networks across 29 Human Tissues. Cell Reports *31*, 107795.

681 Manolio, T.A., Collins, F.S., Cox, N.J., Goldstein, D.B., Hindorff, L.A., Hunter, D.J., McCarthy,
682 M.I., Ramos, E.M., Cardon, L.R., Chakravarti, A., et al. (2009). Finding the missing heritability of
683 complex diseases. Nature *461*, 747–753.

684 Maschietto, M., Bastos, L.C., Tahira, A.C., Bastos, E.P., Euclydes, V.L.V., Brentani, A., Fink, G.,
685 Baumont, A. de, Felipe-Silva, A., Francisco, R.P.V., et al. (2017). Sex differences in DNA
686 methylation of the cord blood are related to sex-bias psychiatric diseases. Sci Rep-Uk *7*, 44547.

687 Molaro, A., Hodges, E., Fang, F., Song, Q., McCombie, W.R., Hannon, G.J., and Smith, A.D.
688 (2011). Sperm Methylation Profiles Reveal Features of Epigenetic Inheritance and Evolution in
689 Primates. Cell *146*, 1029–1041.

690 Morris, A.P., Voight, B.F., Teslovich, T.M., Ferreira, T., Segrè, A.V., Steinthorsdottir, V.,
691 Strawbridge, R.J., Khan, H., Grallert, H., Mahajan, A., et al. (2012). Large-scale association
692 analysis provides insights into the genetic architecture and pathophysiology of type 2 diabetes. Nat
693 Genet *44*, 981–990.

694 Ng, S.-F., Lin, R.C.Y., Laybutt, D.R., Barres, R., Owens, J.A., and Morris, M.J. (2010). Chronic
695 high-fat diet in fathers programs β-cell dysfunction in female rat offspring. Nature *467*, 963–966.

696 Oakes, C.C., Kelly, T.L.J., Robaire, B., and Trasler, J.M. (2007). Adverse Effects of 5-Aza-2′-
697 Deoxycytidine on Spermatogenesis Include Reduced Sperm Function and Selective Inhibition of de
698 Novo DNA Methylation. J Pharmacol Exp Ther *322*, 1171–1180.

699 Oliva, M., Muñoz-Aguirre, M., Kim-Hellmuth, S., Wucher, V., Gewirtz, A.D.H., Cotter, D.J.,
700 Parsana, P., Kasela, S., Balliu, B., Viñuela, A., et al. (2020). The impact of sex on gene expression
701 across human tissues. Science *369*, eaba3066.

702 Peat, J.R., Dean, W., Clark, S.J., Krueger, F., Smallwood, S.A., Ficz, G., Kim, J.K., Marioni, J.C.,
703 Hore, T.A., and Reik, W. (2014). Genome-wide Bisulfite Sequencing in Zygotes Identifies
704 Demethylation Targets and Maps the Contribution of TET3 Oxidation. Cell Reports *9*, 1990–2000.

705 Rodriguez-Terrones, D., and Torres-Padilla, M.-E. (2018). Nimble and Ready to Mingle:
706 Transposon Outbursts of Early Development. Trends Genet *34*, 806–820.

707 Rulands, S., Lee, H.J., Clark, S.J., Angermueller, C., Smallwood, S.A., Krueger, F., Mohammed,
708 H., Dean, W., Nichols, J., Rugg-Gunn, P., et al. (2018). Genome-Scale Oscillations in DNA
709 Methylation during Exit from Pluripotency. Cell Syst *7*, 63-76.e12.

710 Santi, D., Vincentis, S.D., Magnani, E., and Spaggiari, G. (2017). Impairment of sperm DNA
711 methylation in male infertility: a meta-analytic study. Andrology-Us *5*, 695–703.

712 Sherry, S.T., Ward, M.-H., Kholodov, M., Baker, J., Phan, L., Smigielski, E.M., and Sirotkin, K.
713 (2001). dbSNP: the NCBI database of genetic variation. Nucleic Acids Res *29*, 308–311.

714 Singmann, P., Shem-Tov, D., Wahl, S., Grallert, H., Fiorito, G., Shin, S.-Y., Schramm, K., Wolf,
715 P., Kunze, S., Baran, Y., et al. (2015). Characterization of whole-genome autosomal differences of
716 DNA methylation between men and women. Epigenet Chromatin *8*, 43.

717 Smallwood, S.A., Lee, H.J., Angermueller, C., Krueger, F., Saadeh, H., Peat, J., Andrews, S.R.,
718 Stegle, O., Reik, W., and Kelsey, G. (2014a). Single-cell genome-wide bisulfite sequencing for
719 assessing epigenetic heterogeneity. Nat Methods *11*, 817–820.

720 Smallwood, S.A., Lee, H.J., Angermueller, C., Krueger, F., Saadeh, H., Peat, J., Andrews, S.R.,
721 Stegle, O., Reik, W., and Kelsey, G. (2014b). Single-cell genome-wide bisulfite sequencing for
722 assessing epigenetic heterogeneity. Nat Methods *11*, 817–820.

723 Smith, Z.D., Chan, M.M., Mikkelsen, T.S., Gu, H., Gnirke, A., Regev, A., and Meissner, A. (2012).
724 A unique regulatory phase of DNA methylation in the early mammalian embryo. Nature *484*, 339–
725 344.

726 Souza, C.P.E. de, Andronescu, M., Masud, T., Kabeer, F., Biele, J., Laks, E., Lai, D., Ye, P.,
727 Brimhall, J., Wang, B., et al. (2020). Epiclomal: Probabilistic clustering of sparse single-cell DNA
728 methylation data. Plos Comput Biol *16*, e1008270.

729 Takashima, S., Takehashi, M., Lee, J., Chuma, S., Okano, M., Hata, K., Suetake, I., Nakatsuji, N.,
730 Miyoshi, H., Tajima, S., et al. (2009). Abnormal DNA Methyltransferase Expression in Mouse
731 Germline Stem Cells Results in Spermatogenic Defects. Biol Reprod *81*, 155–164.

732 Tang, W.W.C., Dietmann, S., Irie, N., Leitch, H.G., Floros, V.I., Bradshaw, C.R., Hackett, J.A.,
733 Chinnery, P.F., and Surani, M.A. (2015). A Unique Gene Regulatory Network Resets the Human
734 Germline Epigenome for Development. Cell *161*, 1453–1467.

735 Tucci, V., Isles, A.R., Kelsey, G., Ferguson-Smith, A.C., Group, the E.I., Tucci, V., Bartolomei,
736 M.S., Benvenisty, N., Bourc'his, D., Charalambous, M., et al. (2019). Genomic Imprinting and
737 Physiological Processes in Mammals. Cell *176*, 952–965.

738 Uk, A., Collardeau-Frachon, S., Scanvion, Q., Michon, L., and Amar, E. (2018). Assisted
739 Reproductive Technologies and imprinting disorders: Results of a study from a French congenital
740 malformations registry. Eur J Med Genet *61*, 518–523.

741 Vasiliauskaitė, L., Berrens, R.V., Ivanova, I., Carrieri, C., Reik, W., Enright, A.J., and O'Carroll, D.
742 (2018). Defective germline reprogramming rewires the spermatogonial transcriptome. Nat Struct
743 Mol Biol *25*, 394–404.

744 Wen, L., and Tang, F. (2019). Human Germline Cell Development: from the Perspective of Single-
745 Cell Sequencing. Mol Cell *76*, 320–328.

746 WHO (2010). WHO laboratory manual for the examination and processing of human semen,
747 FIFTH EDITION.

748 Wijchers, P.J., and Festenstein, R.J. (2011). Epigenetic regulation of autosomal gene expression by
749 sex chromosomes. Trends Genet *27*, 132–140.

750 Zhou, F., Wang, R., Yuan, P., Ren, Y., Mao, Y., Li, R., Lian, Y., Li, J., Wen, L., Yan, L., et al.
751 (2019). Reconstituting the transcriptome and DNA methylome landscapes of human implantation.
752 Nature *572*, 660–664.

753 Zhu, P., Guo, H., Ren, Y., Hou, Y., Dong, J., Li, R., Lian, Y., Fan, X., Hu, B., Gao, Y., et al.
754 (2018). Single-cell DNA methylome sequencing of human preimplantation embryos. Nat Genet *50*,
755 12–19.

756

Figure 1

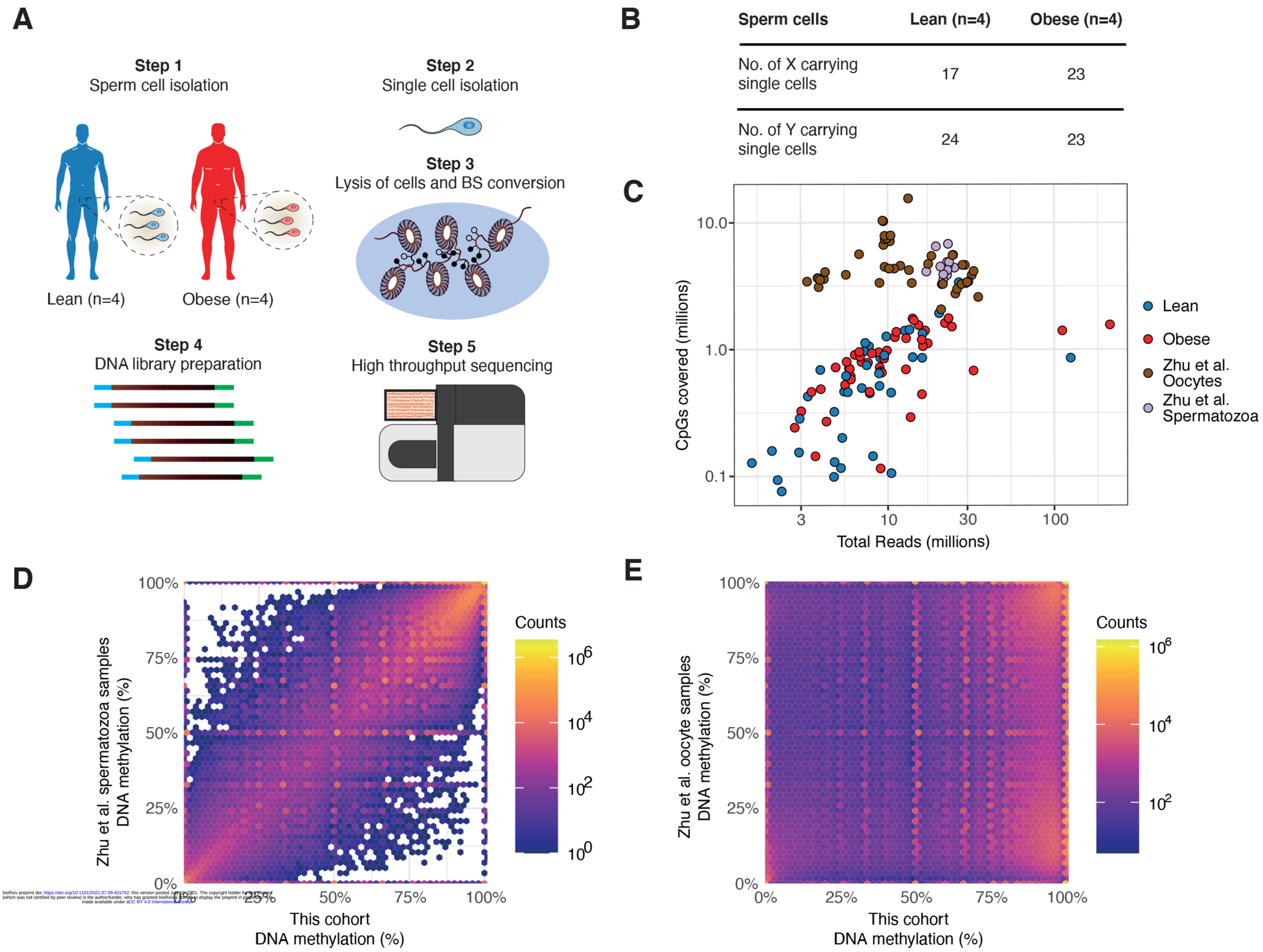

Figure 2

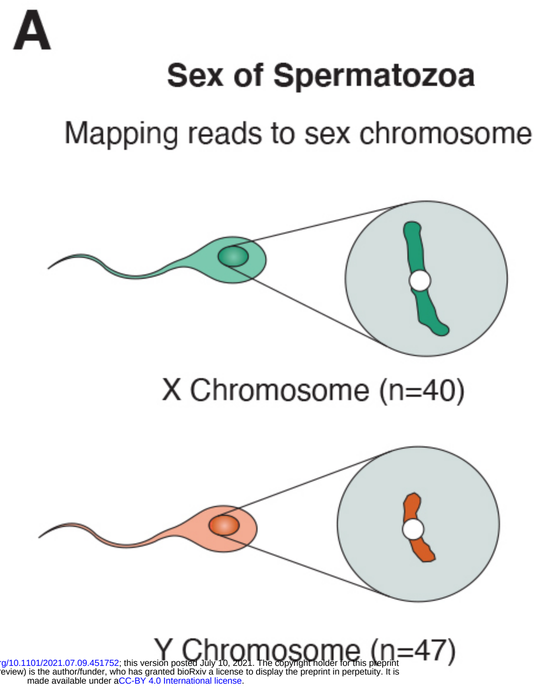

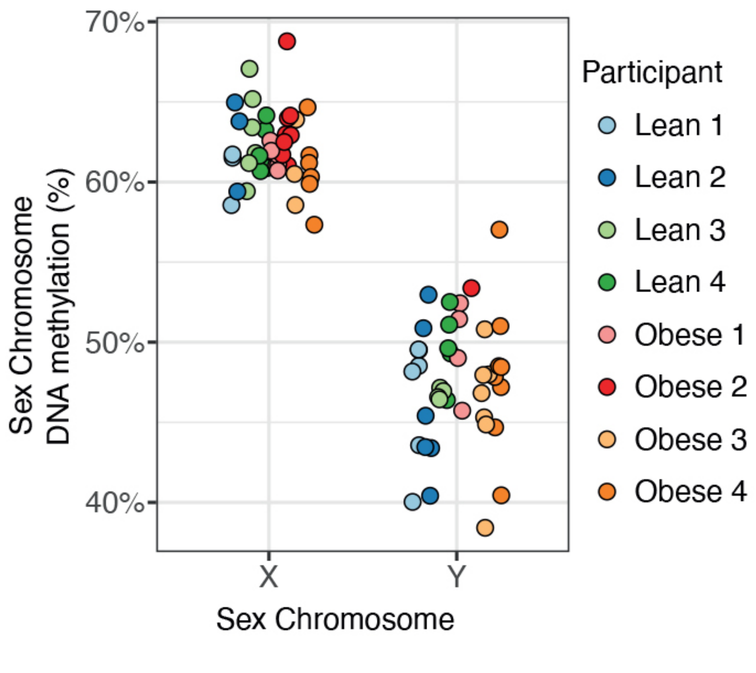

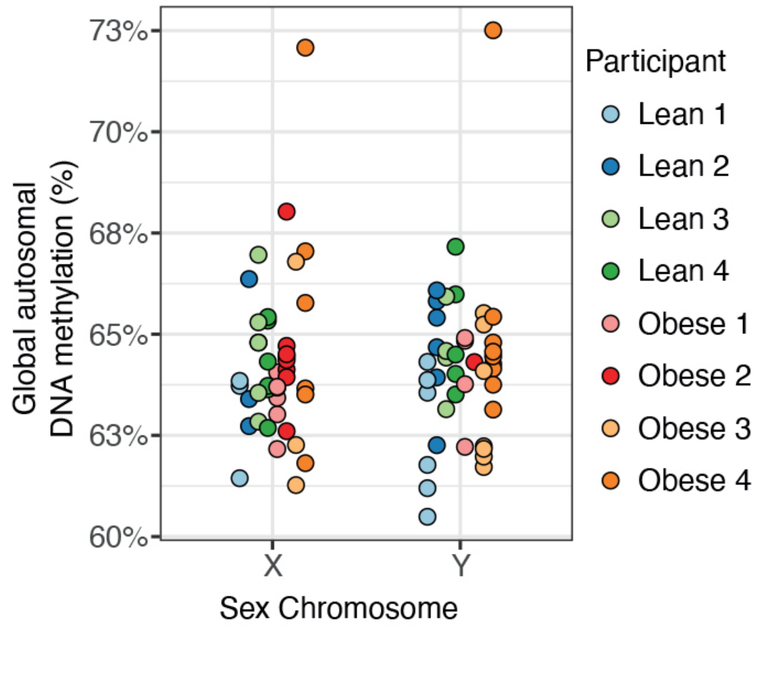

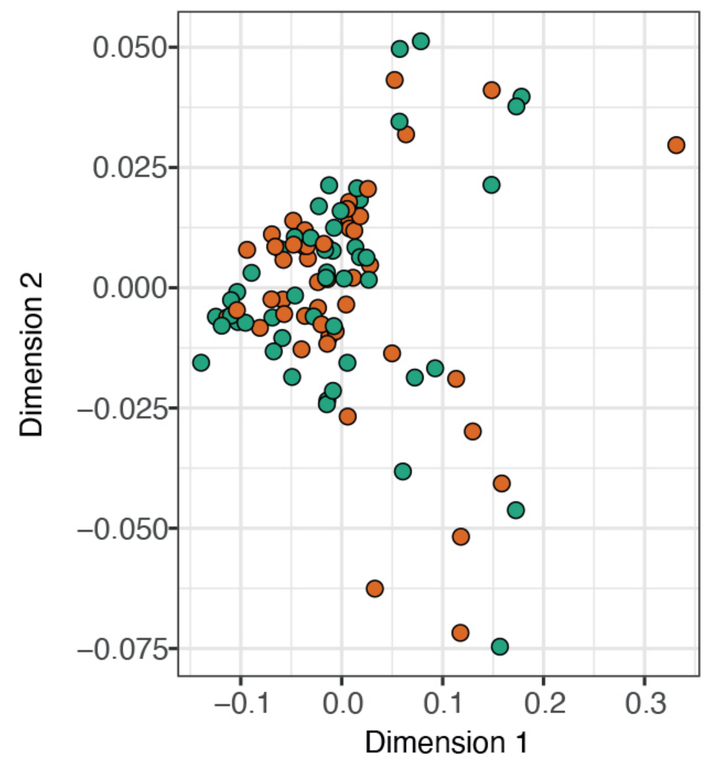

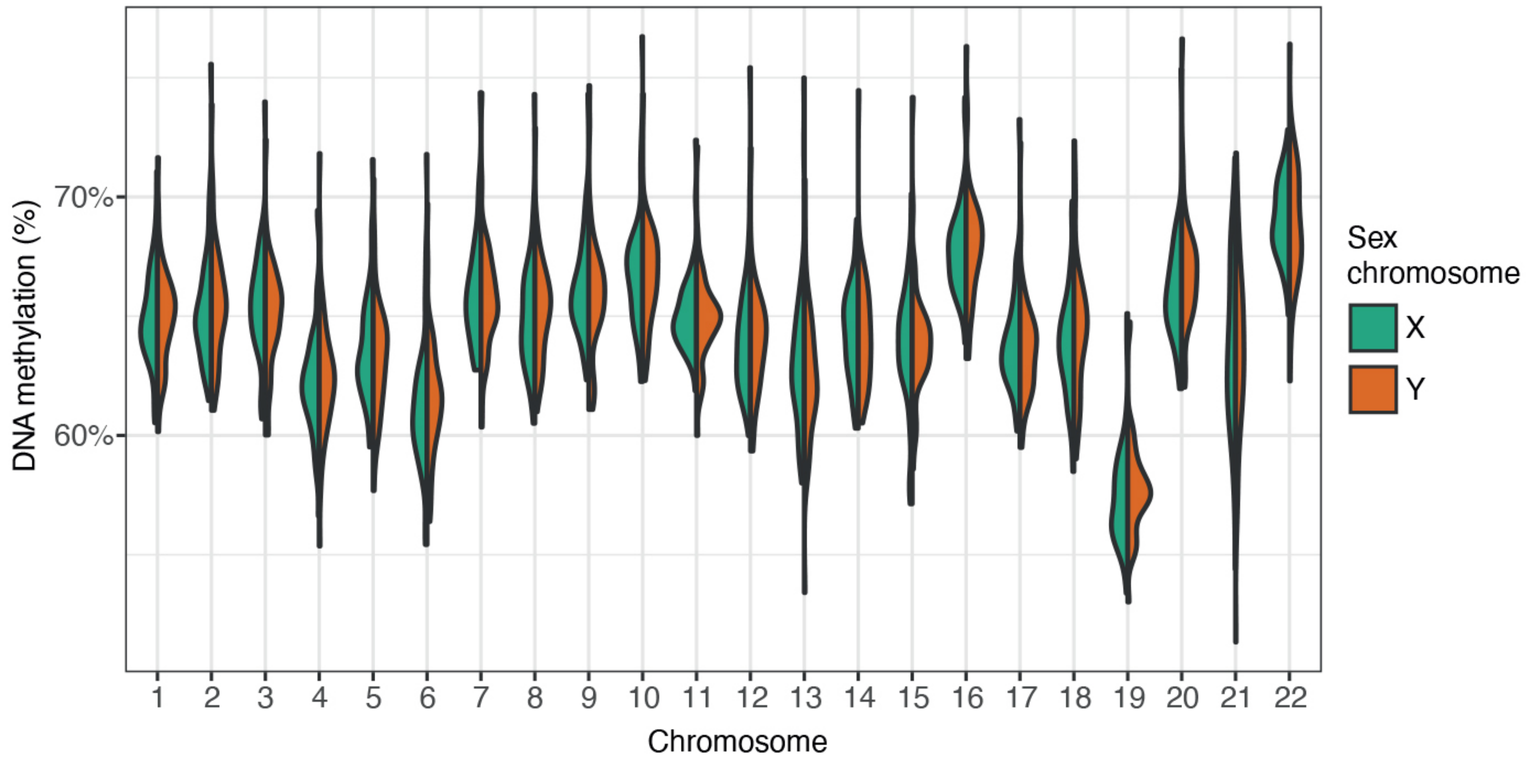

Figure 3

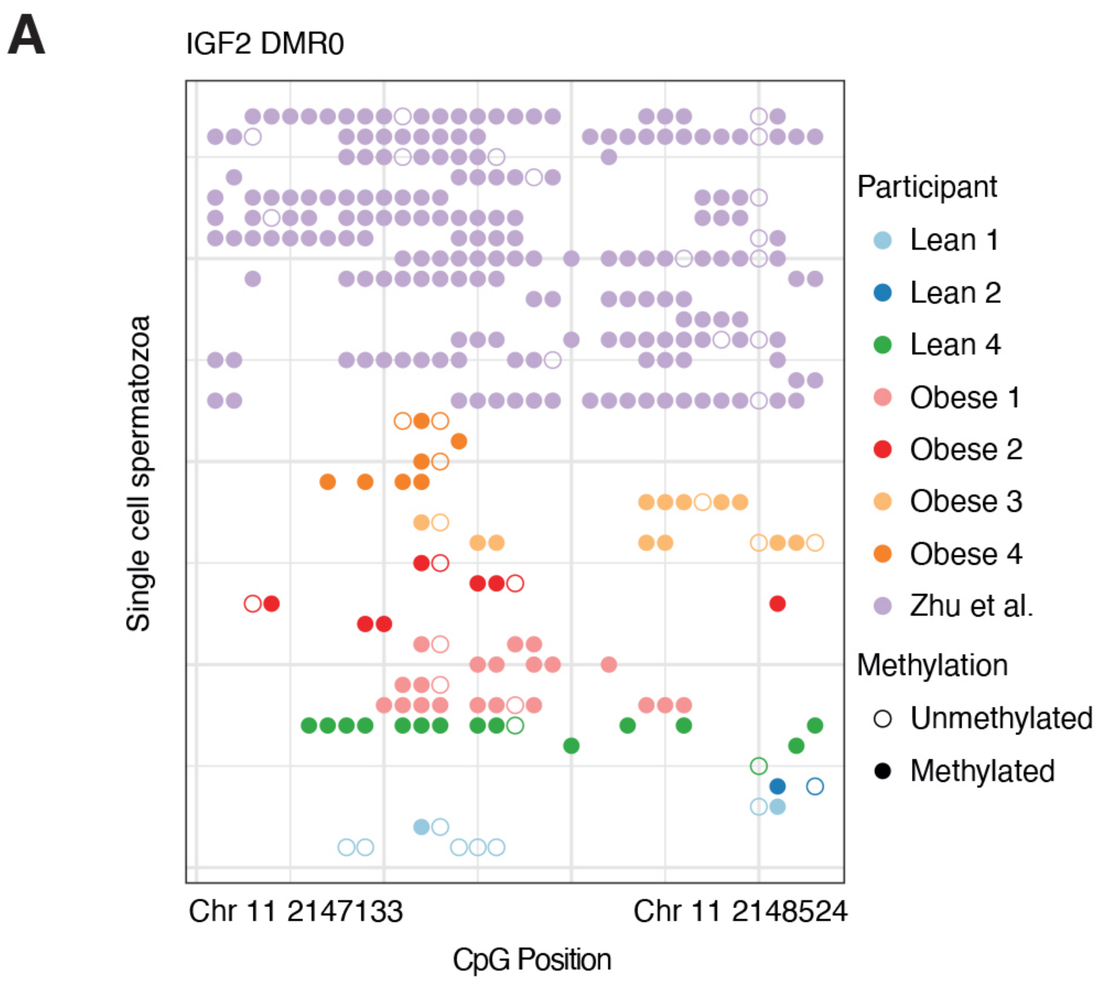

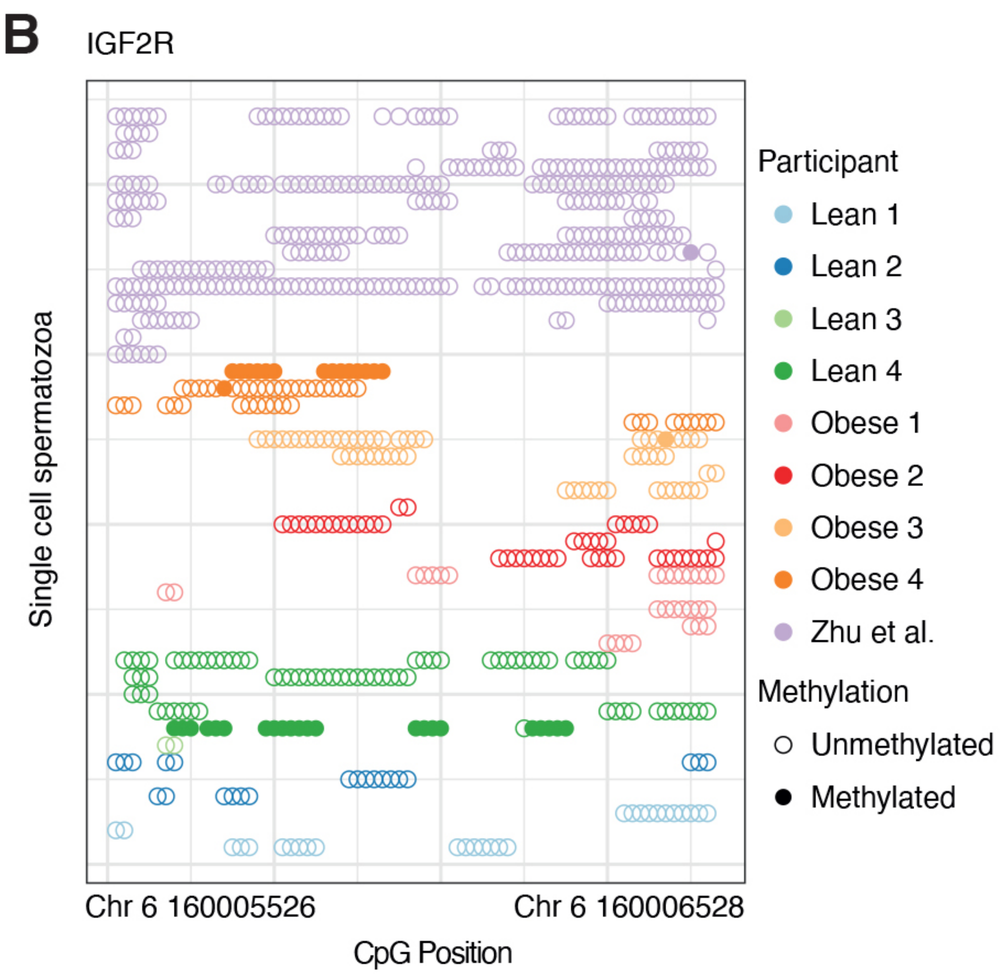

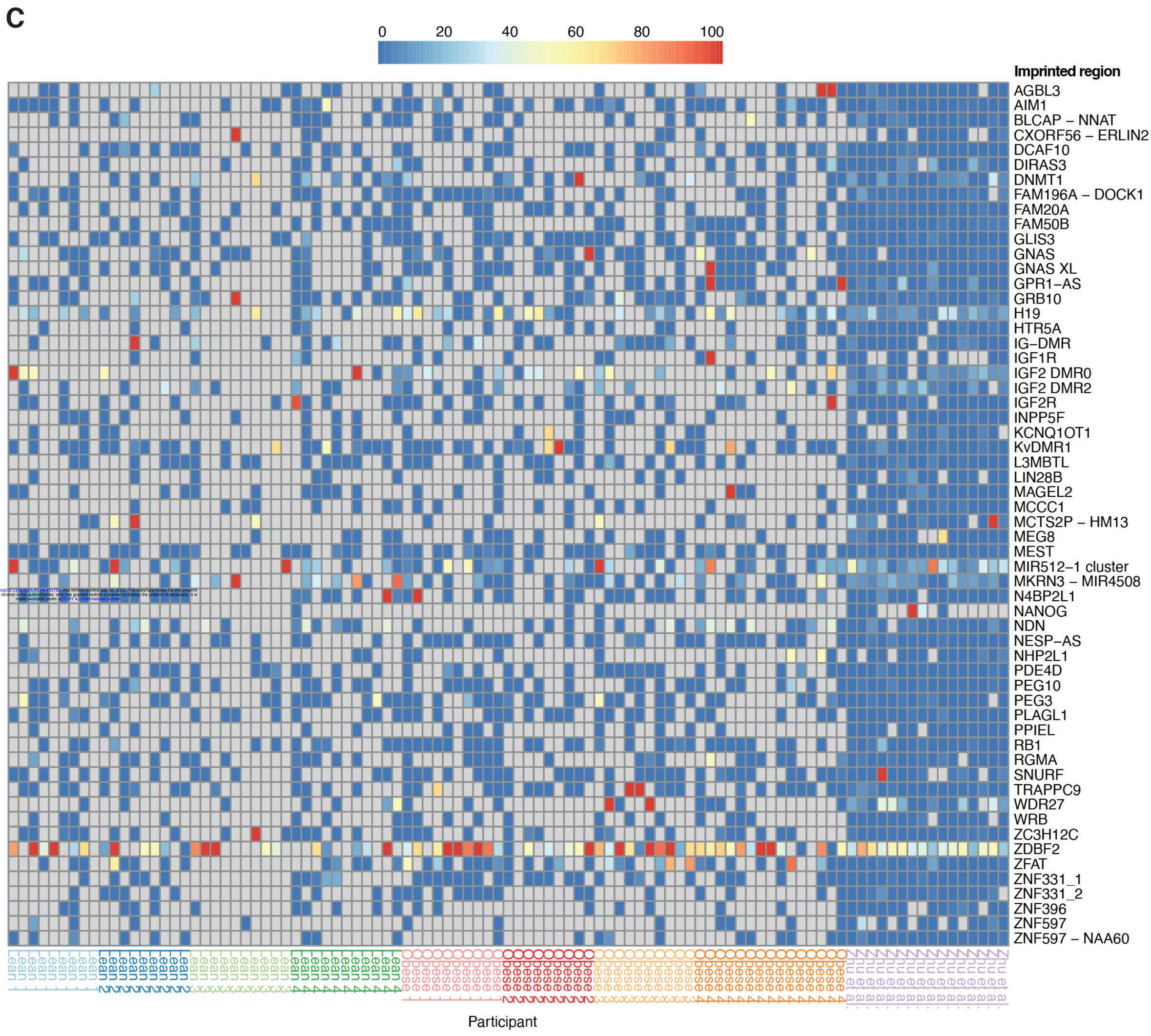

Figure 4

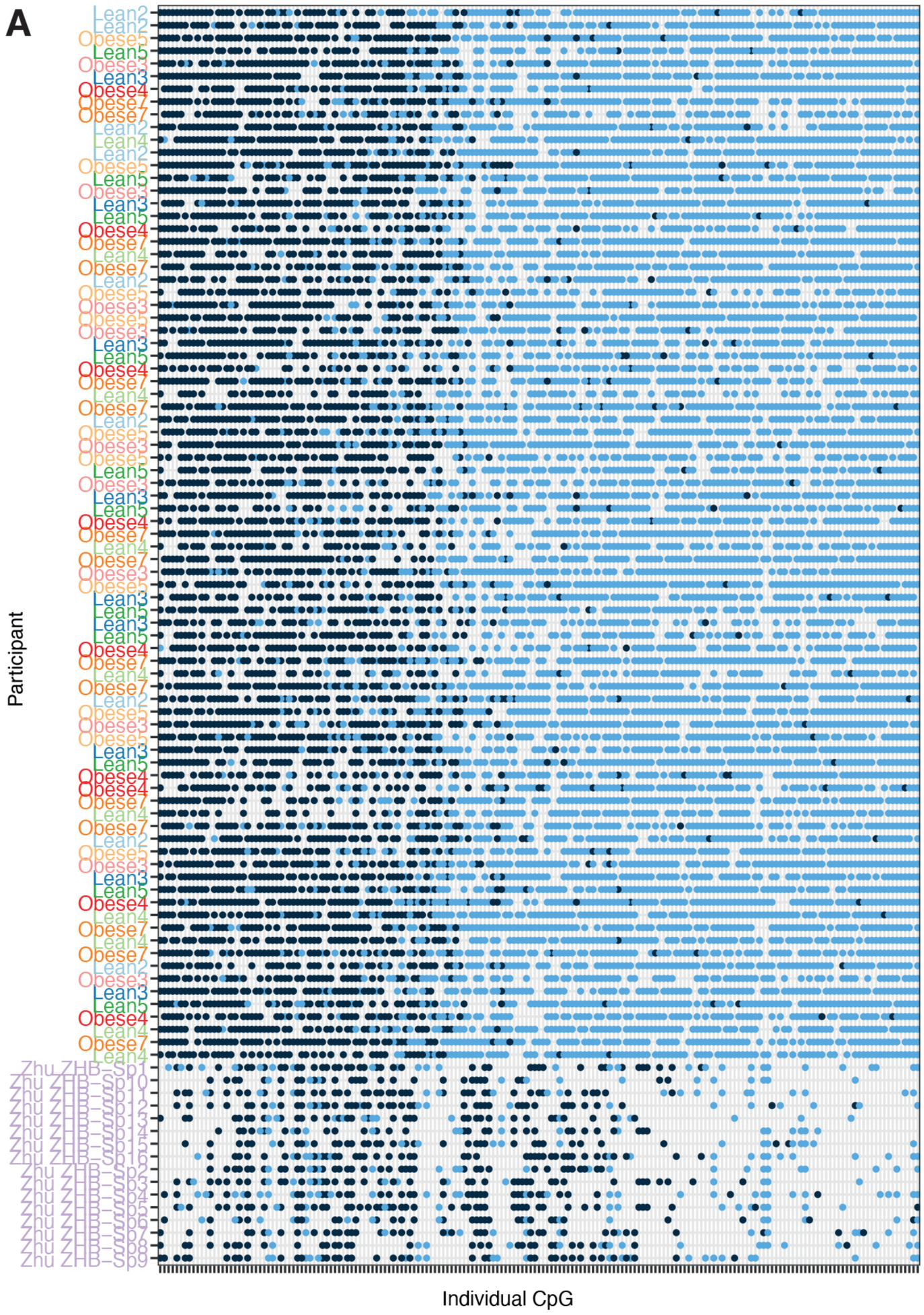

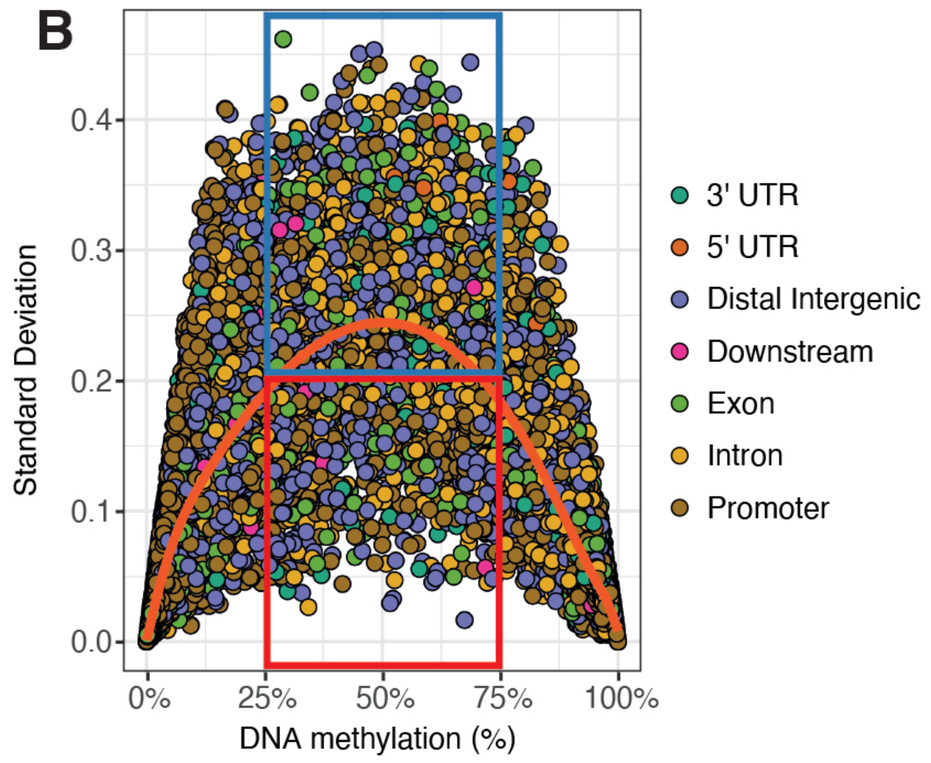

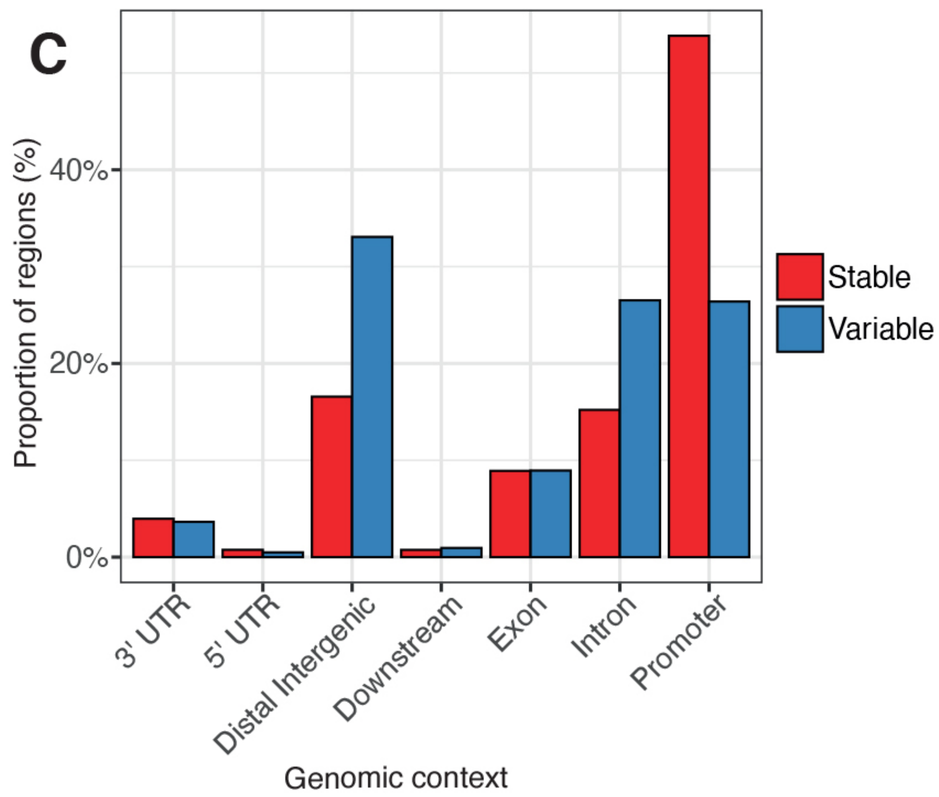

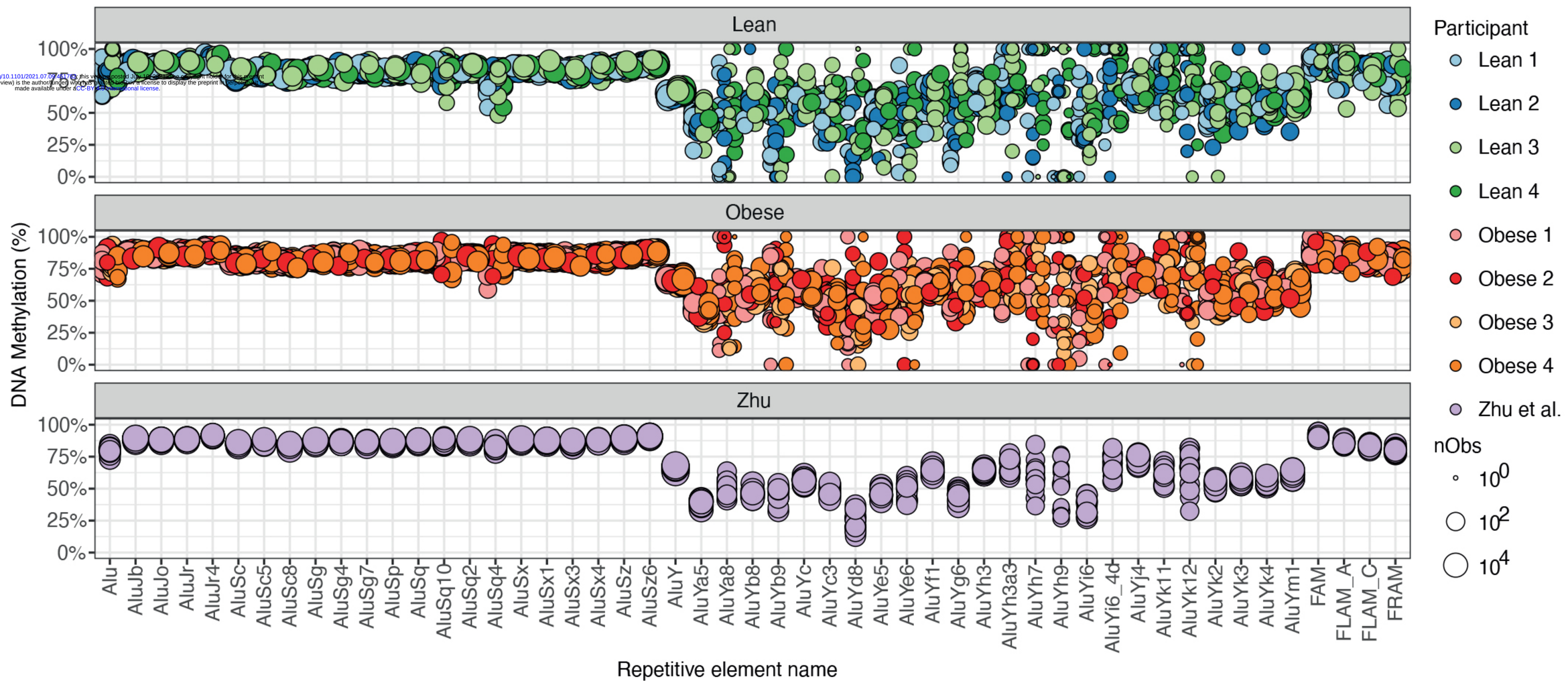

Figure 5

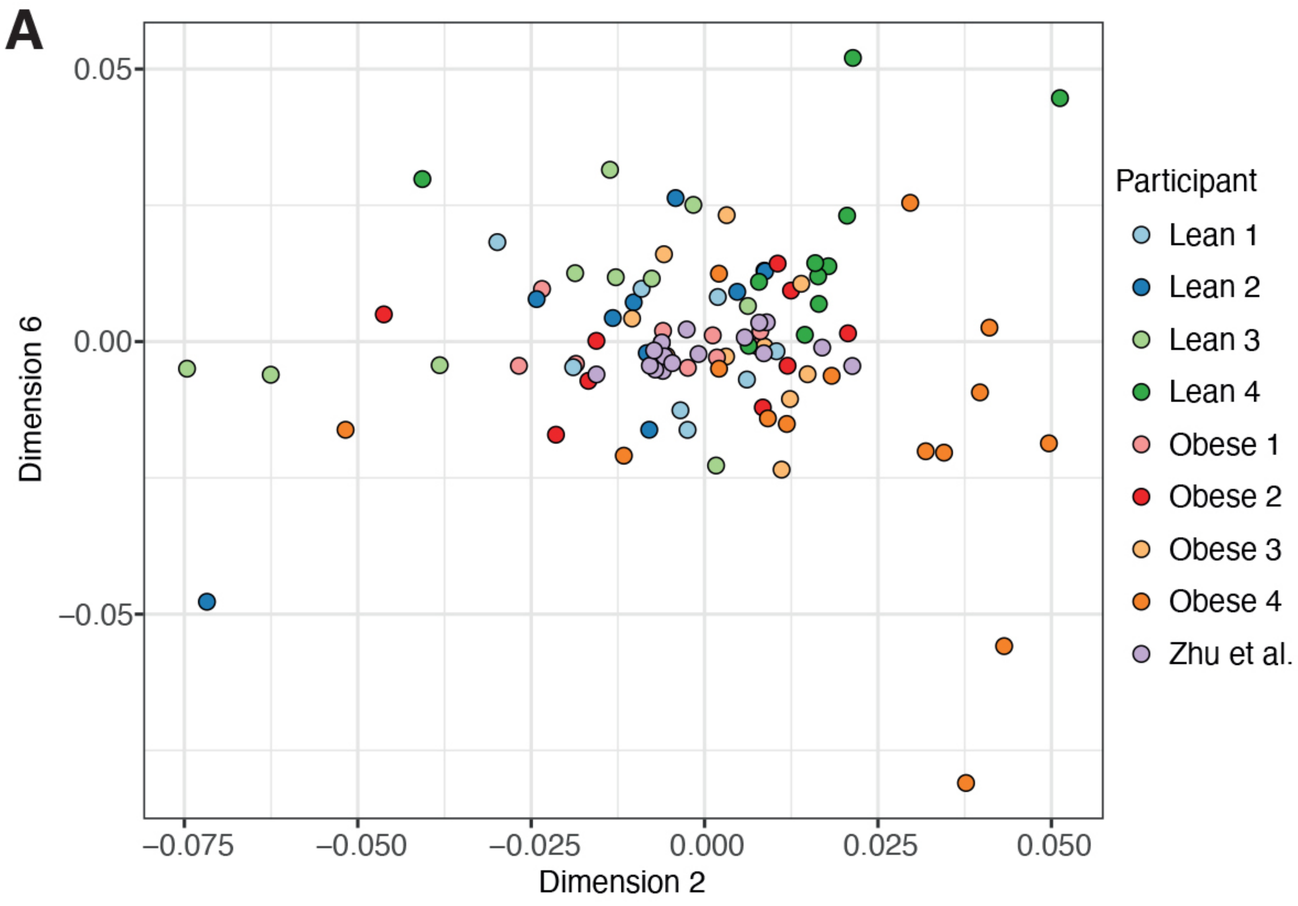

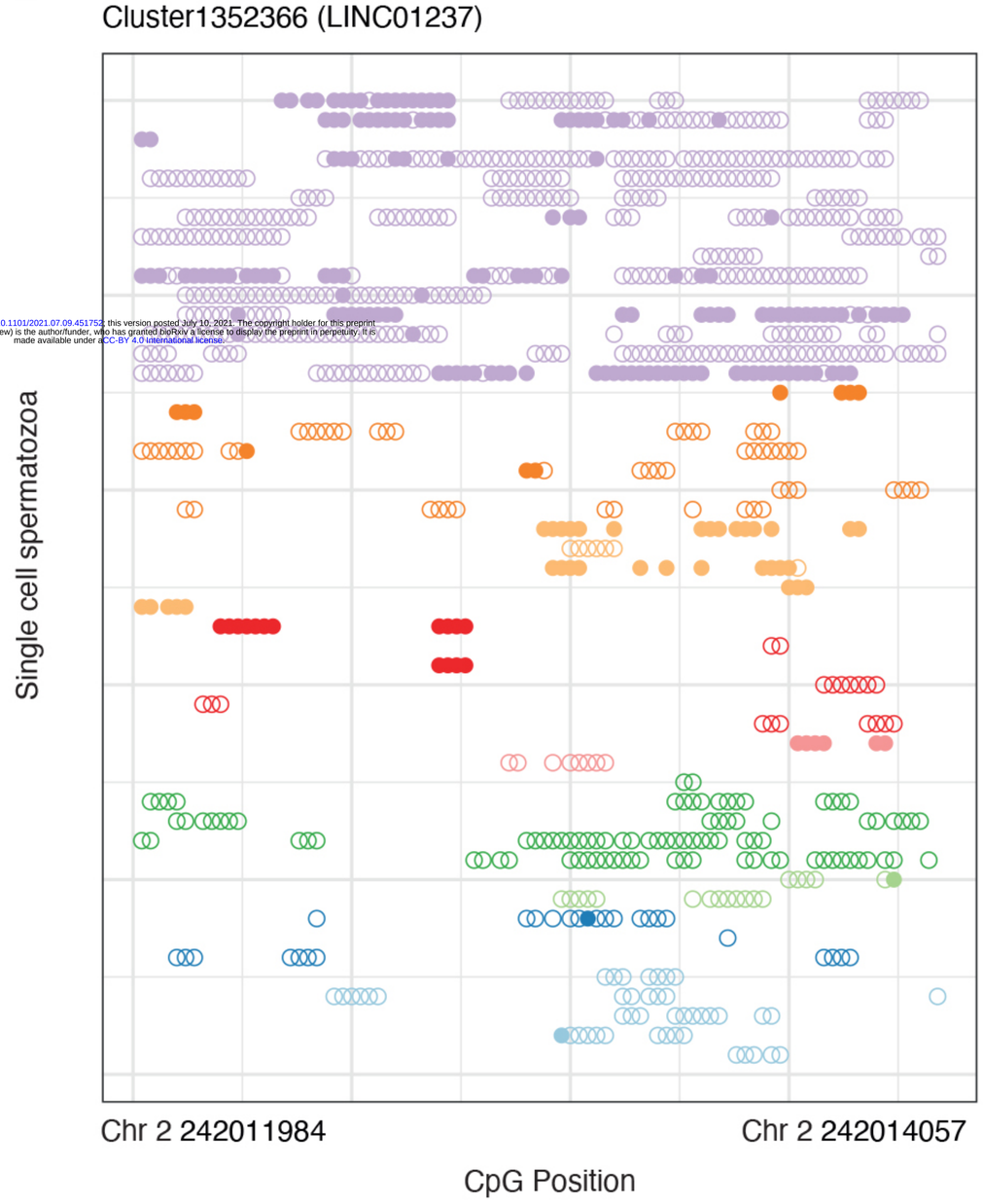

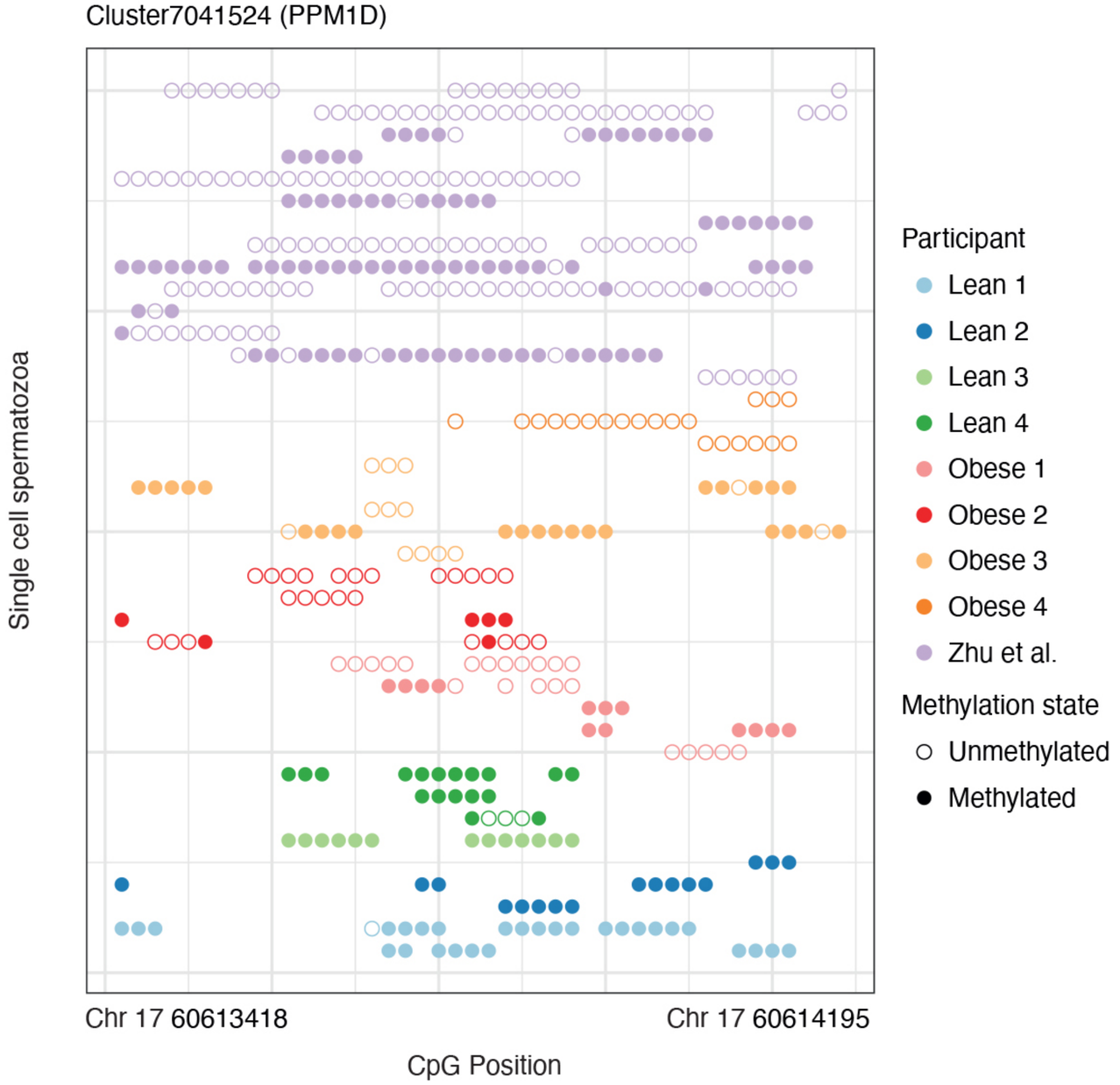

Supplementary figure 1

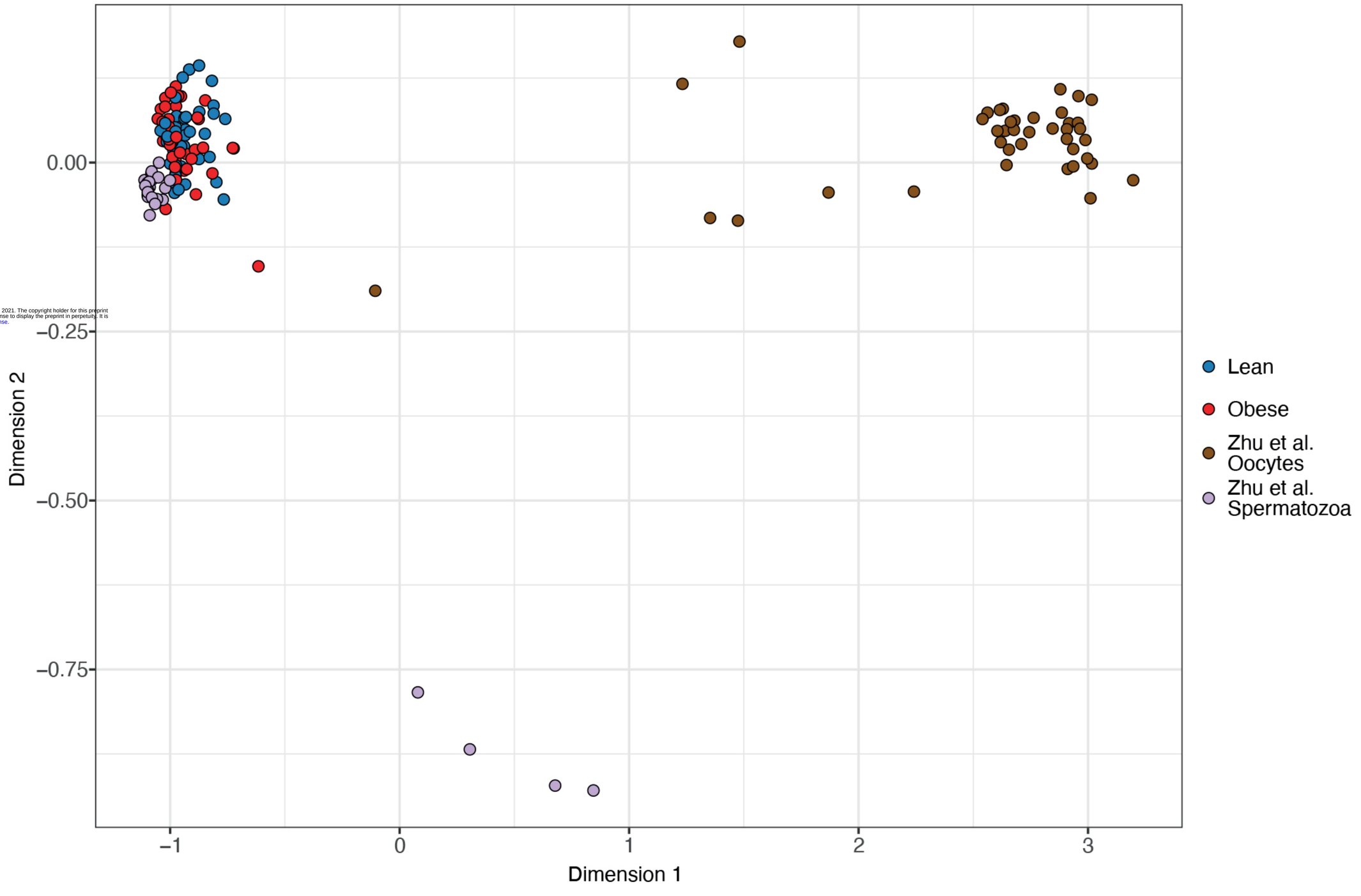

Supplementary figure 2.1

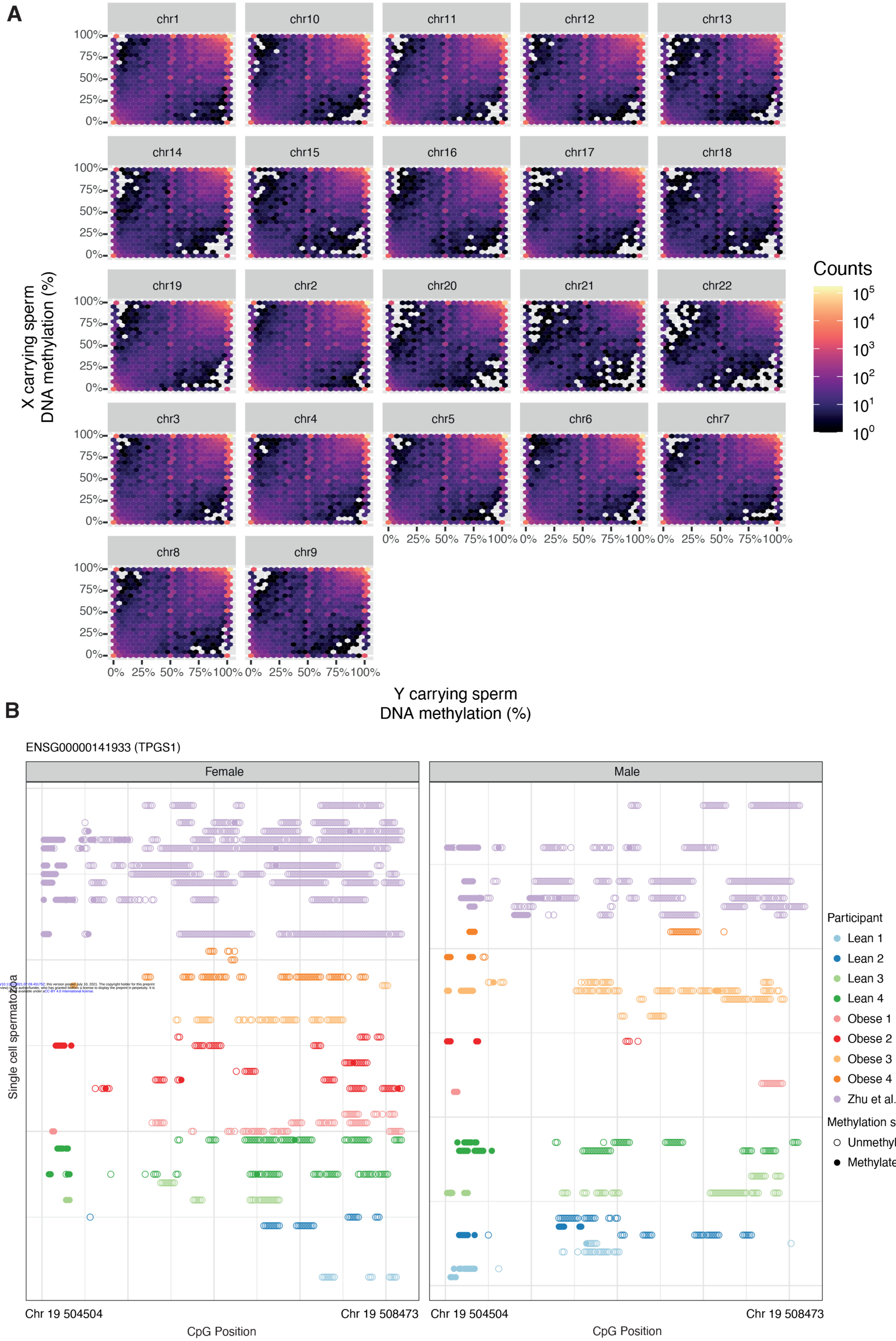

Supplementary figure 2.2

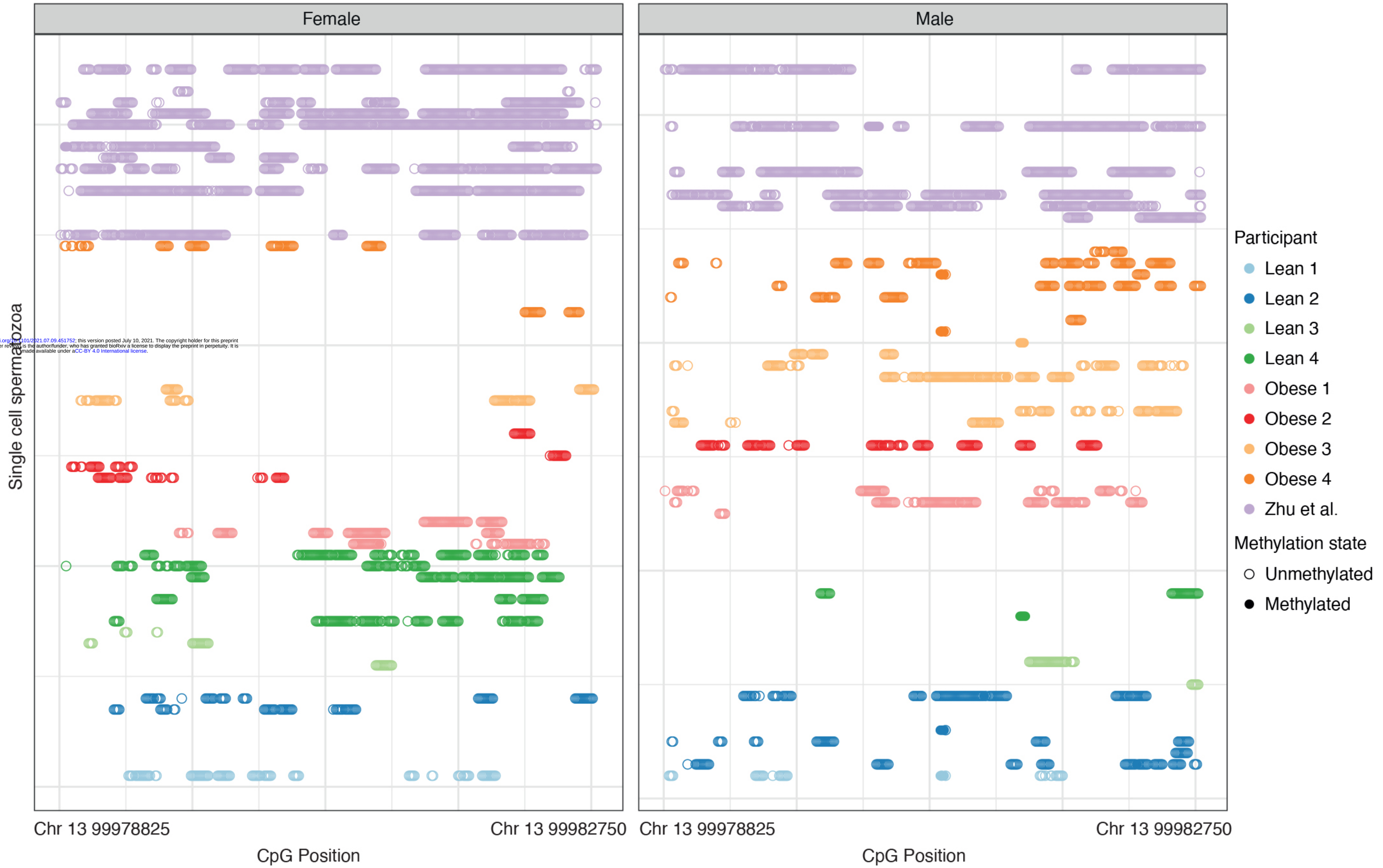

Supplementary figure 3

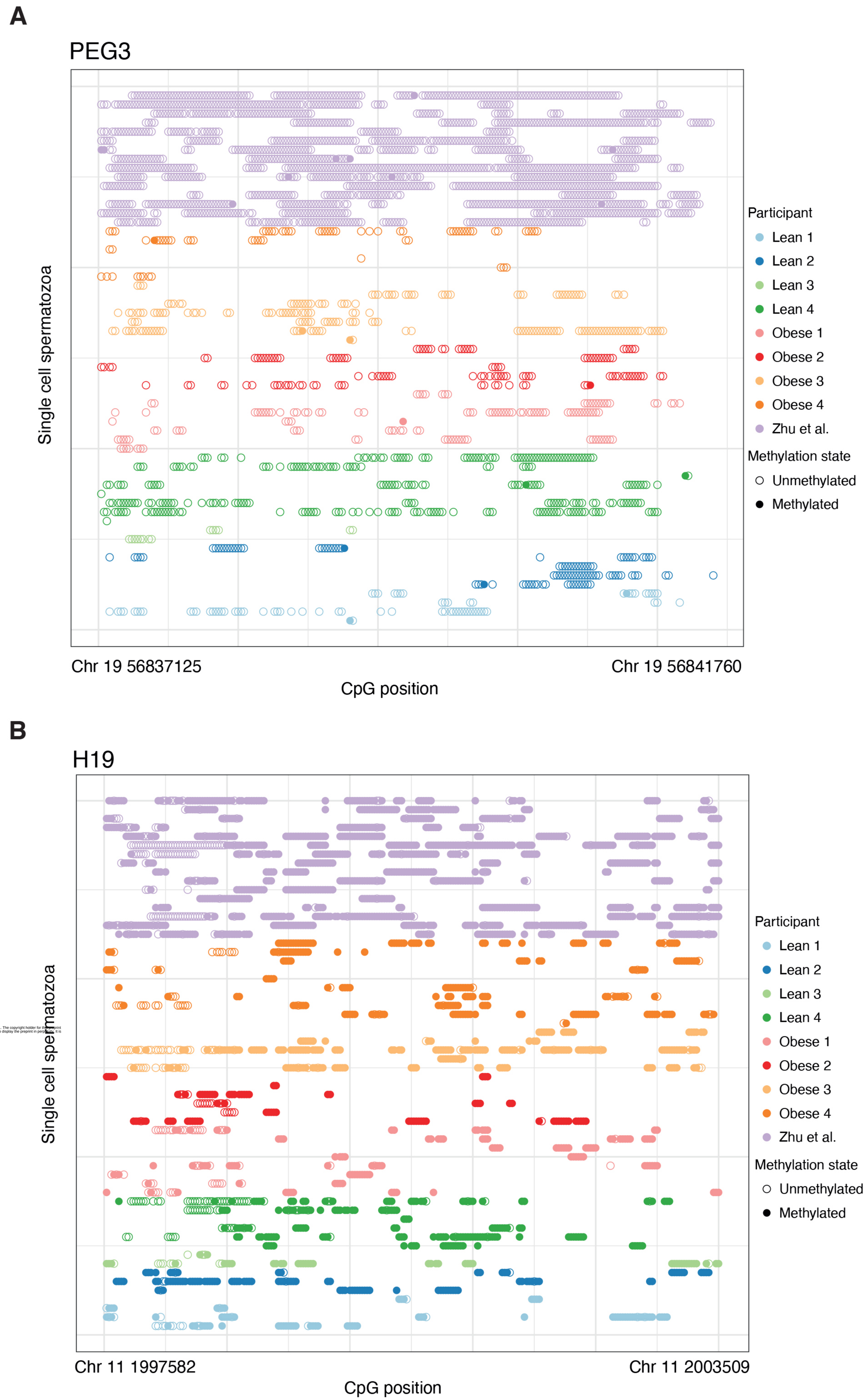

Supplementary figure 4.1

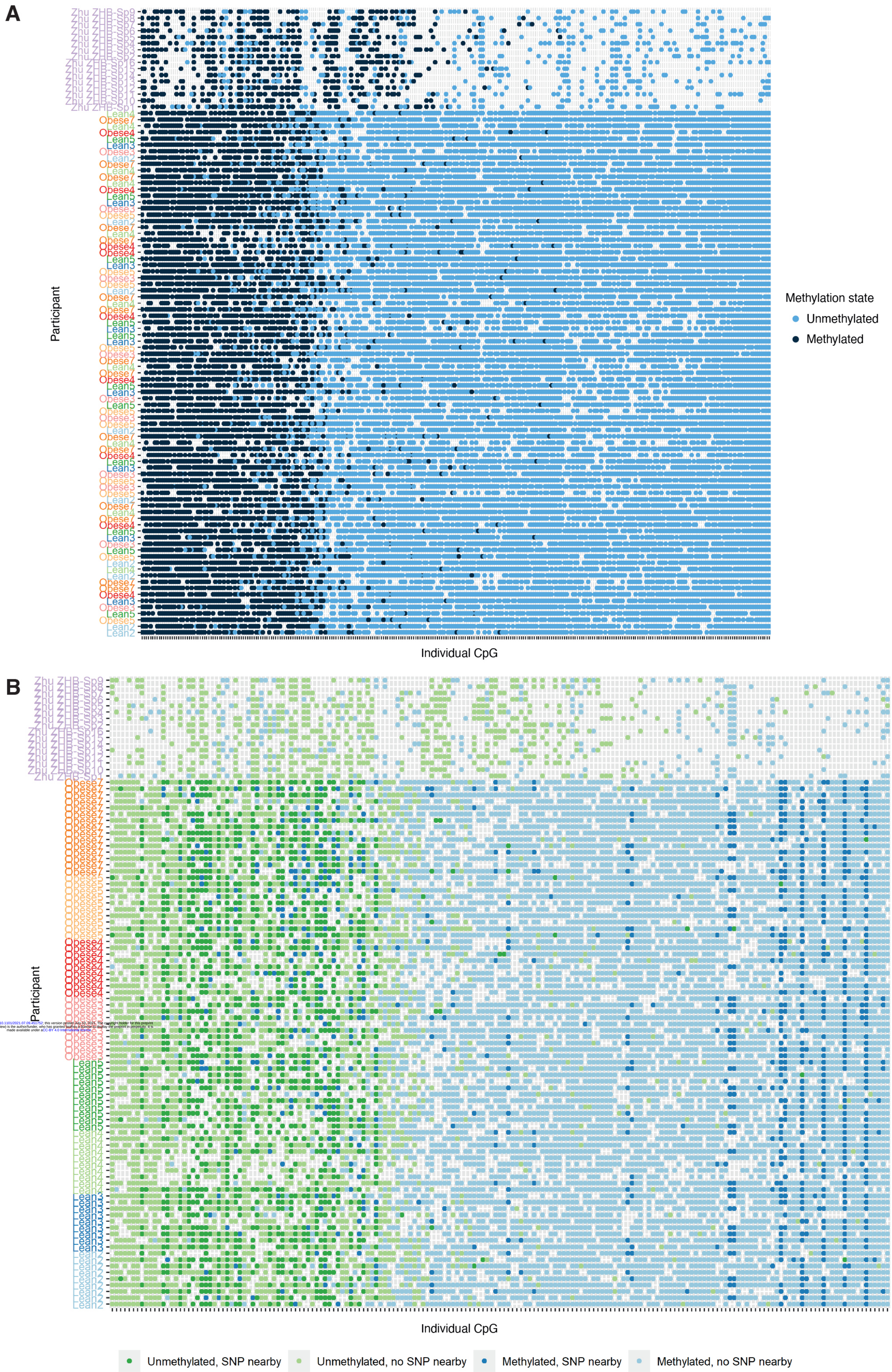

Supplementary figure 4.2

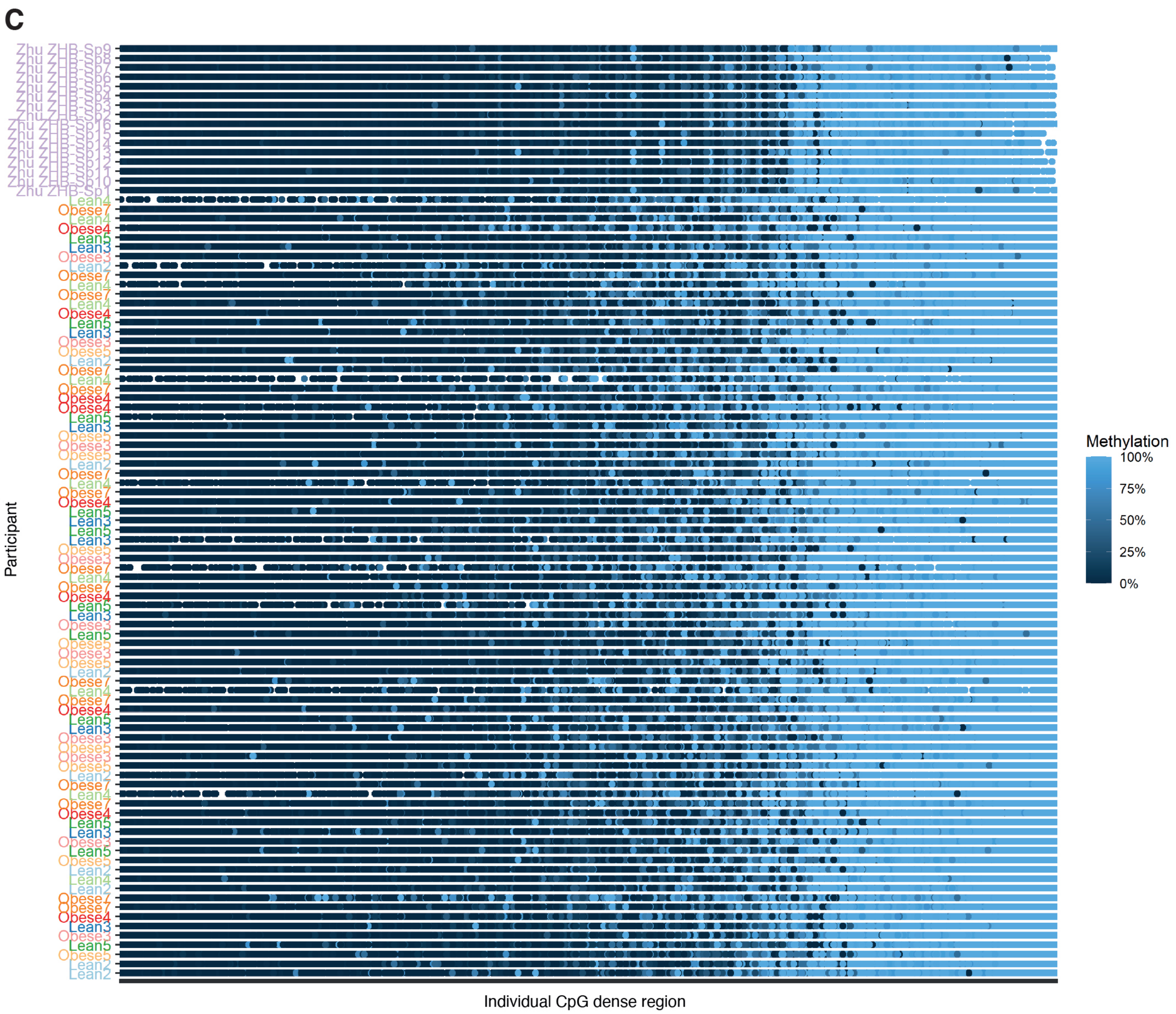

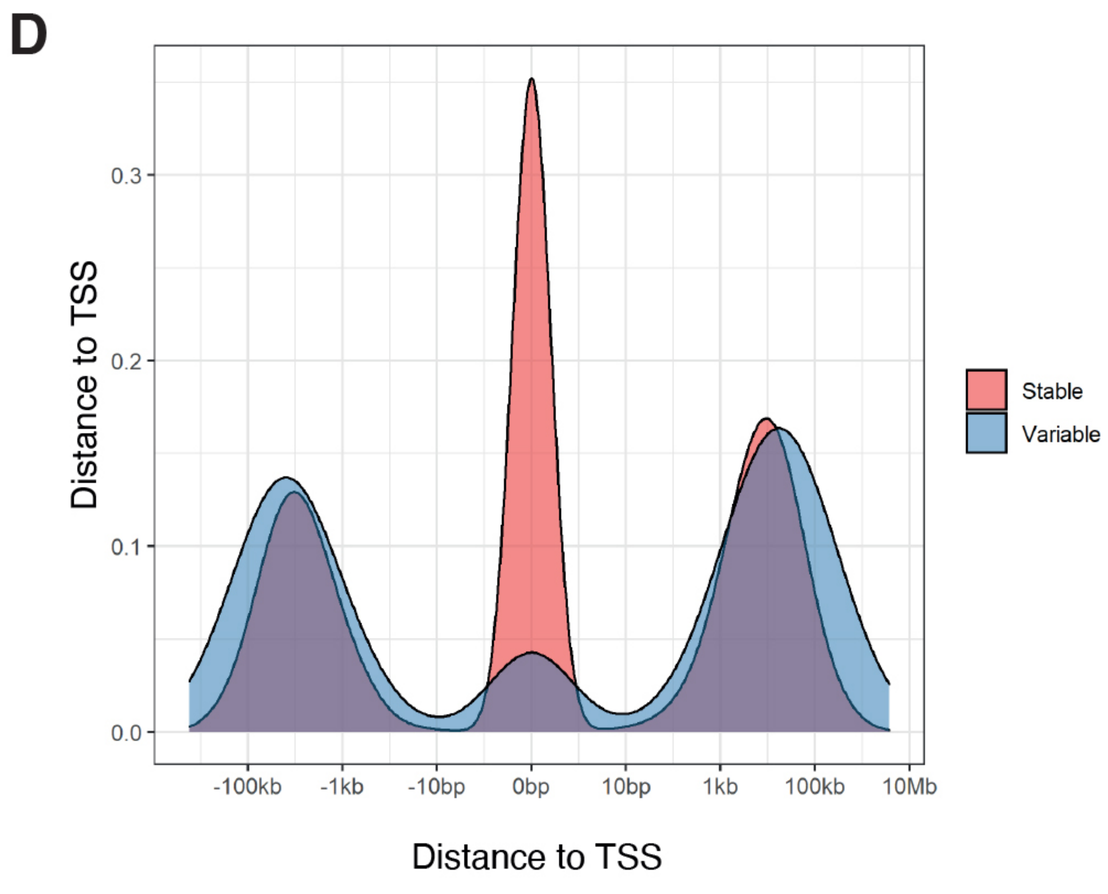

Supplementary figure 4.3

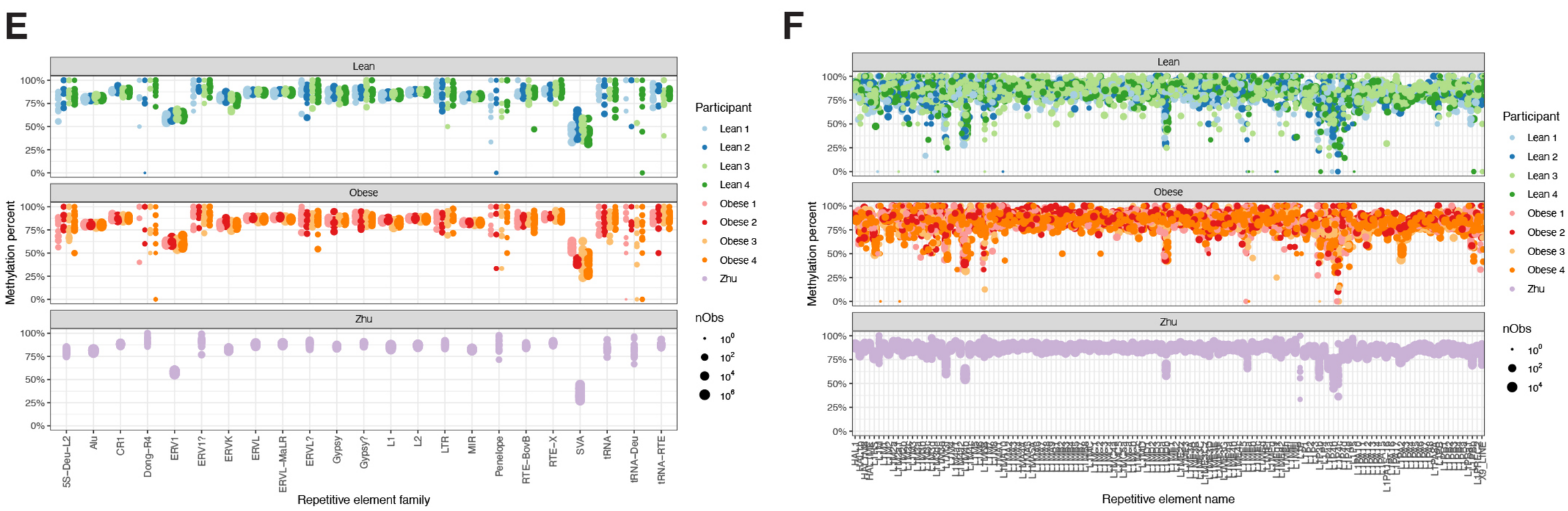

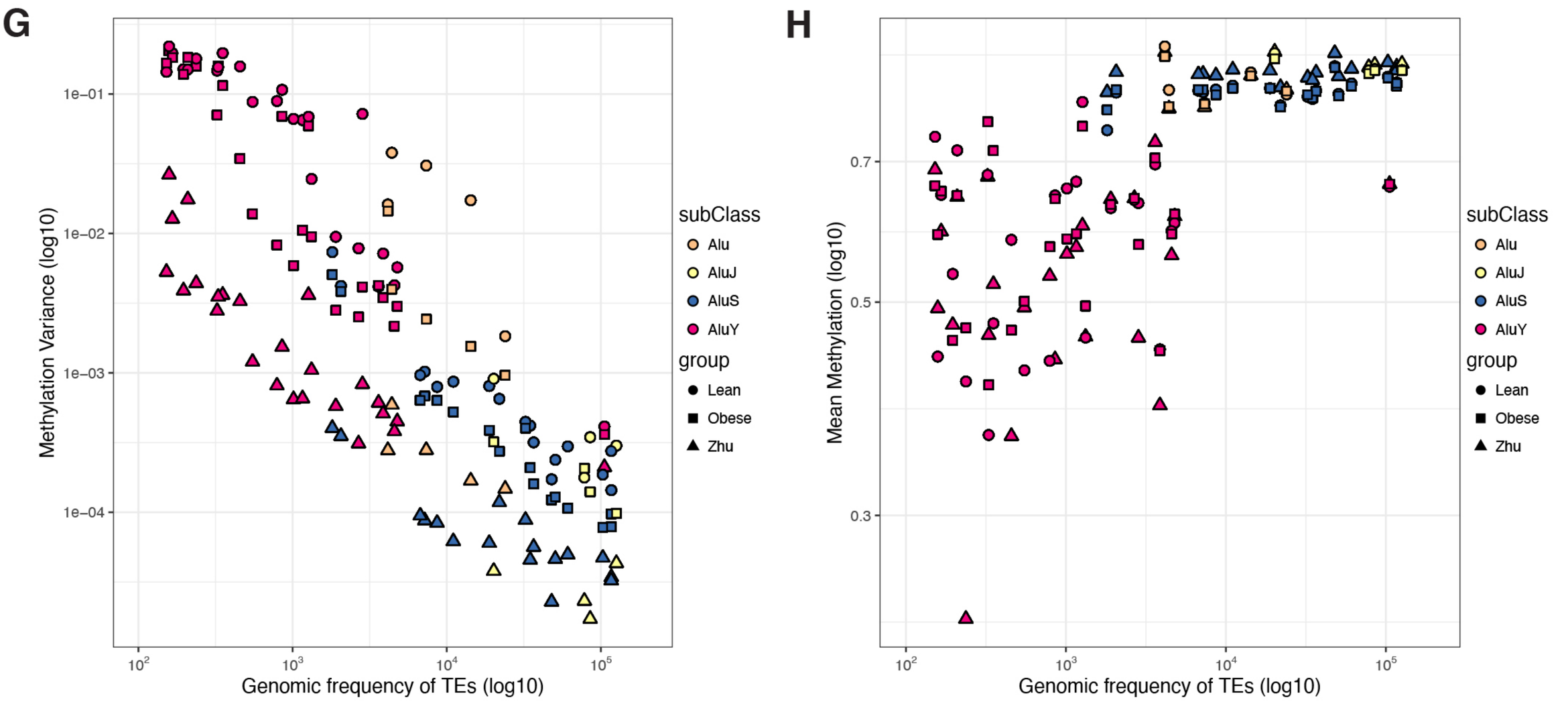

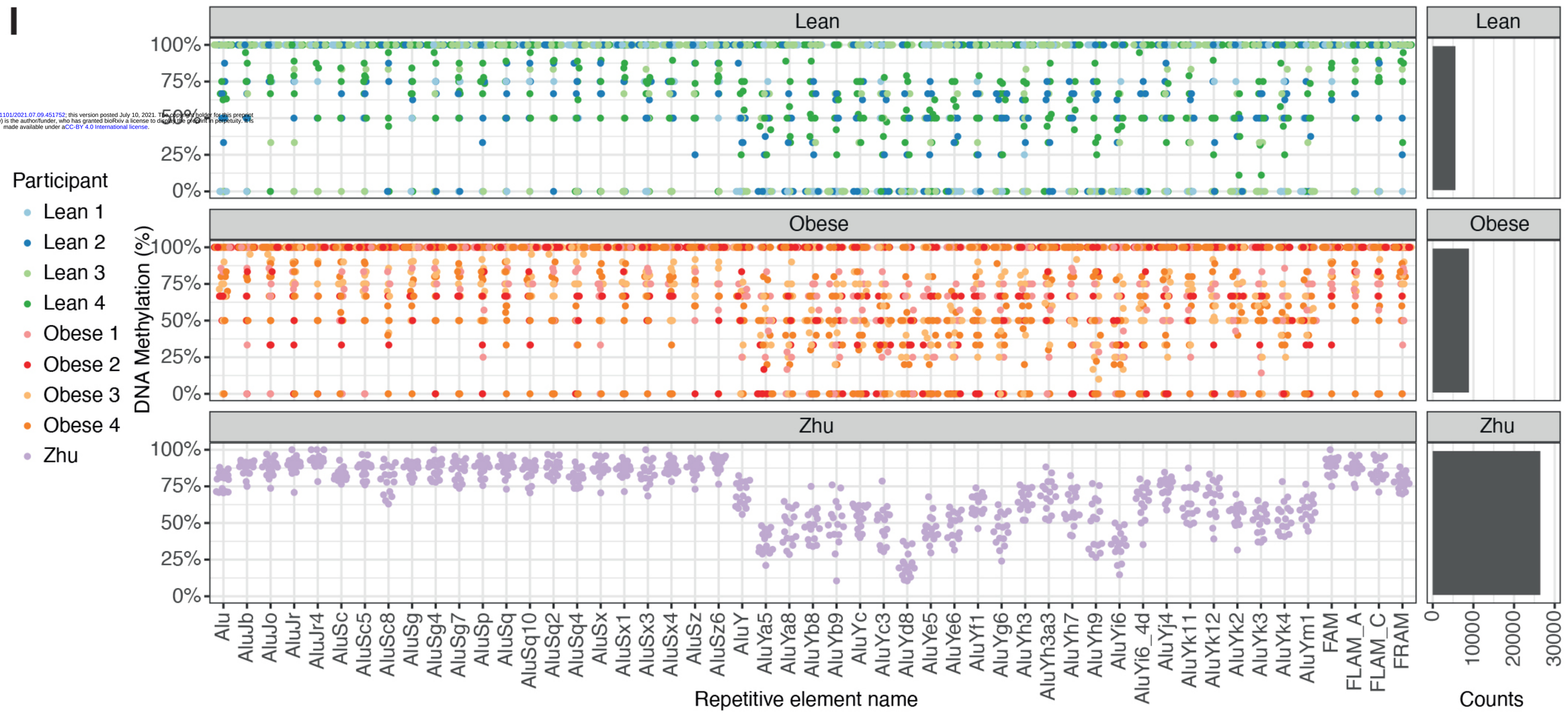

Supplementary figure 5.1

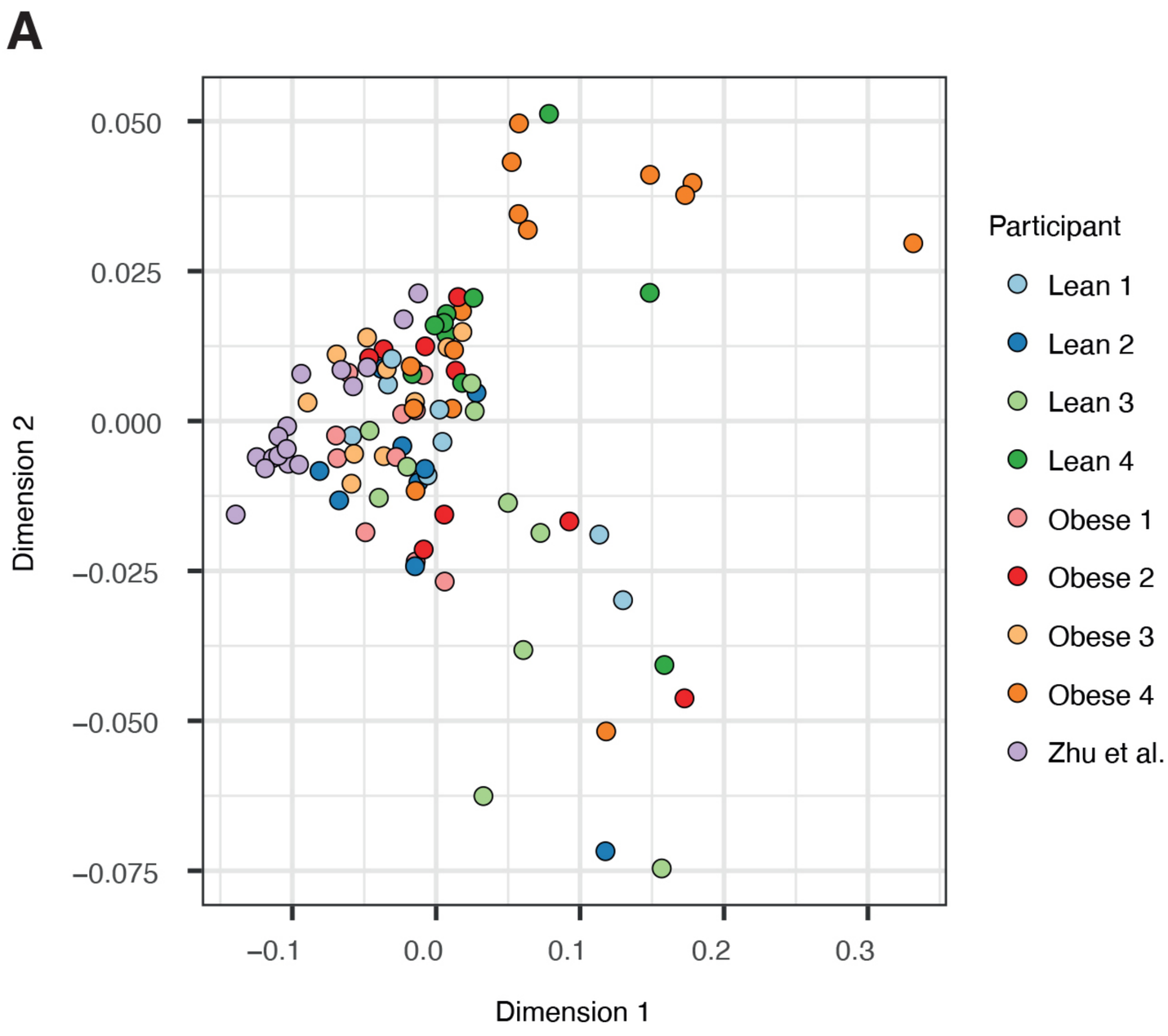

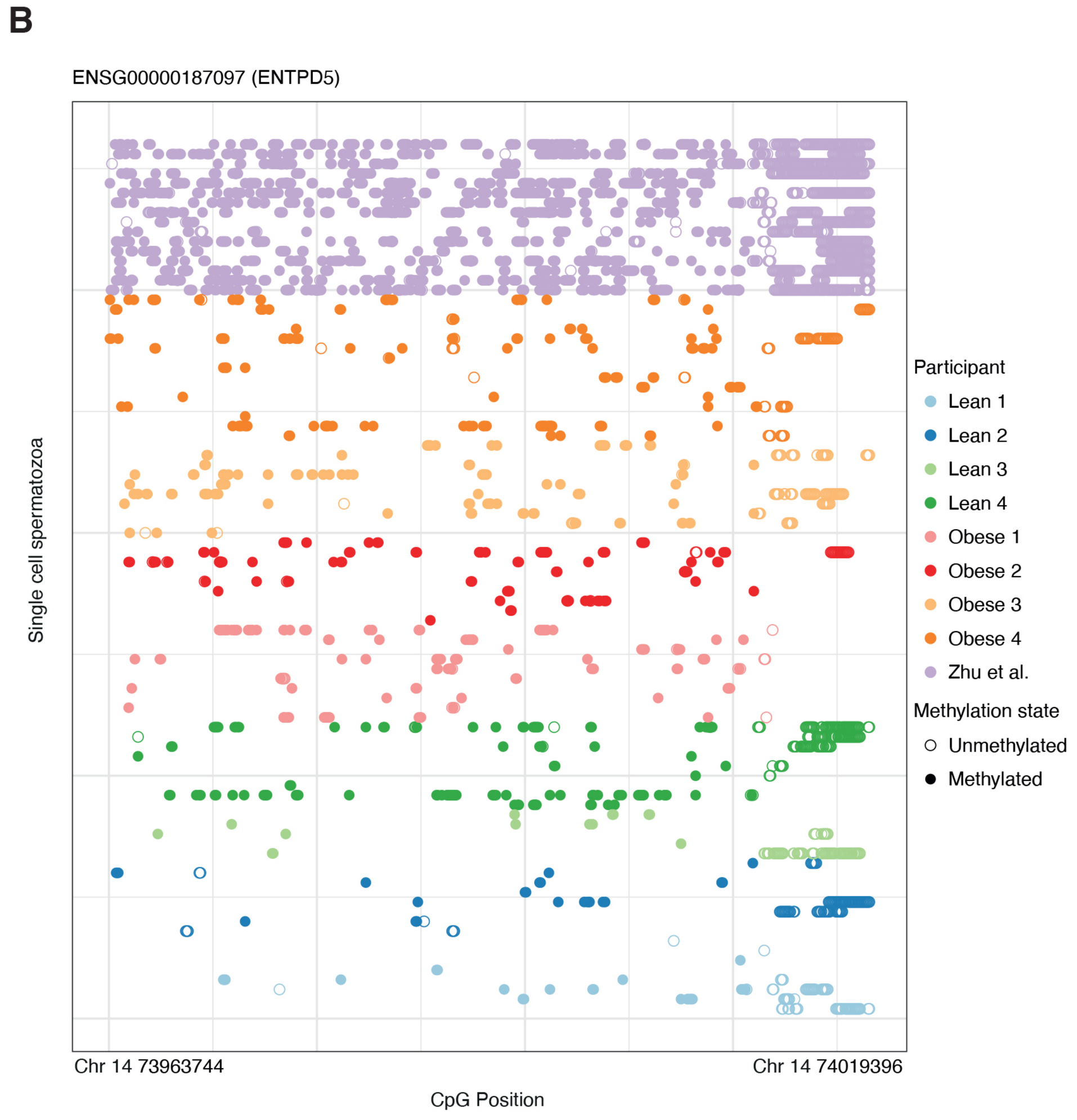

Supplementary figure 5.2